

May 2013
Volume 119
Issue 1925
£5.10

Electronics WORLD

THE ESSENTIAL ELECTRONICS ENGINEERING MAGAZINE
www.electronicsworld.co.uk

Mouser Audio
Applications Site
Inspires Guitar
Audio Revamp



MOUSER
ELECTRONICS.

Technology

SpaceTop3D allows users to
reach inside the computer



From China

Creating a realistic virtual hand
for head-mounted displays



Products

Testers, LED driver ICs,
connectors and much more



Need a True Automotive Expert?

Teledyne LeCroy Automotive Oscilloscopes



Efficient Automotive Design and Debug

Leading Technology

- 8 Channel Solution
- HD4096 True 12-bit Technology:
16x More Vertical Resolution,
Unmatched Measurement Precision
- 36 Digital Channel Mixed Signal Solution

Widest Range of Serial Data Tools

- CAN, LIN, FlexRay™
- MOST, BroadR-Reach, SENT, PSI5
- Manchester & NRZ Configurable Protocol Decode
- I²C, SPI, UART, Ethernet, USB, PCI-Express etc.

teledynelecroy.com/europe

 **TELEDYNE LECROY**
Everywhere you look™

REGULARS

05 TREND

EMERGING CONSUMER APPLICATIONS ARE BOOSTING THE MEMS PRESSURE-SENSOR MARKET

07 TECHNOLOGY

10 THE TROUBLE WITH RF...

THE VITAL 40 MINUTES

by Myk Dormer

36 R&D FROM CHINA

CREATING A REALISTIC VIRTUAL HAND FOR HEAD-MOUNTED DISPLAYS

40 EVENT

ES LIVE

42 EVENT

PCIM EUROPE

44 T&M COLUMN

by Reg Waller

46 PRODUCTS

50 LAST NOTE

Cover prepared by
MOUSER ELECTRONICS
More on pages 8-9

42

Event: PCIM



36

From China:
Design

FEATURES

12

CENTENARY YEAR:
THE FUTURE OF FPGAs –
THE BEST IS YET TO COME

As FPGA provider Altera celebrates 30 years of success in FPGA innovation and development this year, its CTO **Misha Burich** assesses where the FPGA chip technology will go next

14

CENTENARY YEAR:
TRAVELLING AT THE SPEED OF LIGHT

Malcolm Davidson, system and software quality assurance consultant in the offshore oil industry, challenges conventional wisdom of wave propagation, which he calls "the 100-year misunderstanding"

18

IDEAS FOR USING A CHARGE TIME MEASUREMENT
UNIT (CTMU)

Padmaraja Yedamale from Microchip Technology presents 48 applications of how and where to use a Charge Time Measurement Unit (CTMU) to take advantage of its features

24

ACCURATELY PREDICTING PLL REFERENCE SPUR
LEVELS DUE TO LEAKAGE CURRENT

Michel Azarian, Senior Applications Engineer, and Will Ezell, Design Section Lead for Mixed Signal Products at Linear Technology present a simple model for accurately predicting the level of reference spurs due to charge pump and/or op-amp leakage current in a PLL system. Knowing how to predict these levels helps pick loop parameters wisely during the early stages of a PLL system design

32

POWER-SAVING SCHEME FOR VIDEO-ON-DEMAND
SERVICES IN IP TV

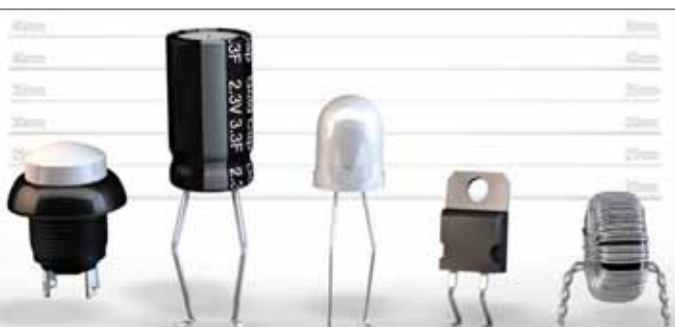
Ikram Syed and Hoon Kim at the University of Incheon in Korea describe an efficient power-saving scheme for VOD services, taking into account the download and playback time of the VOD content

Disclaimer: We work hard to ensure that the information presented in Electronics World is accurate. However, the publisher will not take responsibility for any injury or loss of earnings that may result from applying information presented in the magazine. It is your responsibility to familiarise yourself with the laws relating to dealing with your customers and suppliers, and with safety practices relating to working with electrical/electronic circuitry – particularly as regards electric shock, fire hazards and explosions.



Make us part of your electronics line-up.
FIND IT. DESIGN IT. BUY IT.

rswww.com/electronics



Combining two worlds. Audio analysis plus HDMI functionality.

In Blu-ray™ player, TV or AV receiver production, it's not just important to analyze video quality. You also have to check audio quality. But you don't always need high-end analyzers designed for complex R&D issues, and you don't want to have one box for audio and another for video analysis. The R&S®UPP is the answer, with 100 % audio analysis plus basic video test functionality for HDMI interfaces. It's the combination of performance and value you've been looking for.

Interested?

www.rohde-schwarz.com/ad/upp



EMERGING CONSUMER APPLICATIONS ARE BOOSTING THE MEMS PRESSURE-SENSOR MARKET

After years of limited growth, the MEMS pressure-sensor market has taken off again at a healthy 22% CAGR, this time due to their use in consumer electronics applications.

Pressure sensors are playing an important role in modern-day industries as they are widely adopted in different applications because of their high performance, low cost and small size. The MEMS pressure sensor was one of the very first MEMS components to appear in various microsystems. Today this is a large market that is also rather mature. But, French-based market research firm Yole Développement expects it to be buoyed anew by the consumer market, growing from \$1.9bn in 2012 to \$3bn in 2018.

"The MEMS pressure-sensor for consumer applications, especially for smartphones and tablets, is following the model of accelerometers and gyroscopes," said Wenbin Ding, Technology & Market Analyst for MEMS Devices and Technologies at Yole Développement. "Adoption of this model will help the MEMS pressure-sensor market boom again."

Ding added: "We believe this huge opportunity will result in the global volume of the MEMS pressure-sensor market hitting 2.8 billion units by 2018. Of this pressure sensors for consumer applications will represent 1.7 billion units and will overtake automotive as the market leader in volume."

Automotive applications still dominate the MEMS pressure-sensor market. Tyre Pressure Monitoring Systems (TPMS), manifold absolute pressure (MAP) sensors and barometric air pressure (BAP) sensors will be the biggest sub-applications in this field. Automotive, medical, industrial and high-end markets are growing 4% to 7%, whereas the consumer market is growing

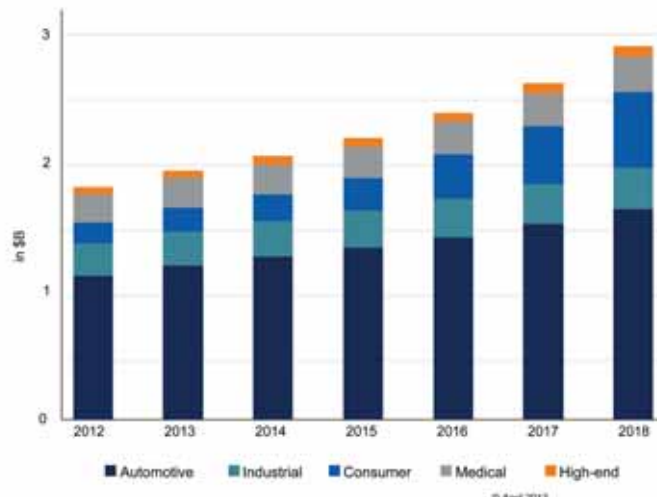


We believe this huge opportunity will result in global volume of the MEMS pressure-sensor market hitting 2.8 billion units by 2018

25% in value (38% in volume) because of new opportunities in smartphones and tablets.

"Even though the consumer application has a much lower ASP than other applications, this promising segment will bring more than 8% CAGR to the global MEMS pressure-sensor market," said Ding.

Yole Développement has prepared a report on this subject, entitled 'MEMS Pressure Sensor', in which it gives a detailed overview of these devices, their markets and applications, and the key players. Industries covered include automotive, industrial, medical applications, consumer electronics and high-end (aeronautical, military, defense).



MEMS pressure sensor market forecast by applications 2012-2018

(Source : MEMS Pressure Sensor report, April 2013, Yole Développement)

Yole Développement was founded in 1998, and today has grown to become a group of companies providing marketing, technology and strategy consulting, in addition to corporate finance services, with a strong focus on emerging applications that use silicon

EDITOR: Svetlana Josifovska
+44 (0)1732 883392
Email: svetlanaj@sjpbusinessmedia.com

DESIGN: Tania King
Email: taniak@sjpbusinessmedia.com

DISPLAY SALES: John Steward
Tel: +44 (0)20 7933 8974
Email: johns@sjpbusinessmedia.com

SALES EXECUTIVE: Orla Cullen
Tel: +44 (0)20 7933 8999
Email: orlac@sjpbusinessmedia.com

PUBLISHER: Wayne Darroch

ISSN: 1365-4675

PRINTER: Pensorad Magazines & Periodicals

SUBSCRIPTIONS:
Tel/Fax +44 (0)1635 879361/868594
Email: electronicsworld@circdata.com

SUBSCRIPTION RATES:
1 year: £56 (UK); £81 (worldwide)



Follow us on Twitter
@electrowo



Join us on LinkedIn
<http://linkd.in/xH2HNx>

ANALOG INTEGRATION ISN'T FOR EVERYONE



www.maximintegrated.com

SEE-THROUGH COMPUTERS ARE EXPECTED IN GENERAL USE WITHIN A DECADE



The SpaceTop 3D computer allows users to reach inside to manipulate files

Massachusetts Institute of Technology (MIT) graduate Jinhua Lee, supported by Microsoft, has developed a transparent computer that allows users to reach inside it to manipulate and work with files, documents and 3D models.

Called SpaceTop 3D desktop, the design was inspired by our need to

interact with things directly, and it is expected to make computing easier and more intuitive.

"It is one of our key human skills to be able to interact with 3D spaces and I wanted to let people do the same with digital content. Spatial memory, where the body intuitively remembers where things are, is a very human

skill," said Lee. "[With SpaceTop 3D] if you are working on a document you can pick it up and flip through it like a book."

"The gap between what the designer thinks and what the computer can do is huge. If you can put your hands inside the computer and handle digital content you can express ideas more completely," he added.

The system consists of a transparent LED display with built-in cameras, which track the user's gestures and eye movements. For more

precise tasks, where hand gestures are less accurate, a touchpad can still be used.

Future interfaces will be developed to distinguish differences between textures and details, or indeed allow a user to grip things of various shapes and sizes. Translating everyday touch into the digital world will enable people to use computers more easily as well as complete more complex tasks.

The basic SpaceTop model is expected to come into general use within a decade.

Researchers Finally Crack the Mystery of the 1/f Noise in Electronics Systems

Researchers at the University of California say they have solved an almost century-old problem that could further help downsize electronic devices. The work led by Alexander Balandin, a professor of electrical engineering at UC Riverside, targeted the low-frequency electronic 1/f noise, also known as pink or flicker noise. It is a signal with a power spectral density inversely proportional to the frequency. It was first discovered in vacuum tubes in 1925 and since then it has been found everywhere, from fluctuations of the intensity in music recordings, to heart rates, as well as electrical currents in materials and devices.

A question of particular importance for electronics was whether 1/f noise was generated on the surface of electrical conductors or inside

them. This motivated numerous studies of its physical origin and methods for its control. For example, the signal's phase noise in radar or a communication gadget such as a smartphone is to a large degree determined by the 1/f noise level in the transistors used in them. But until now, the origin of 1/f noise in most of systems remained a mystery.

The team of researchers from the UC Riverside, Rensselaer Polytechnic Institute (RPI) and Ioffe Physical-Technical Institute of The Russian Academy of Sciences used a set of multi-layered graphene samples with the thickness continuously varied from one atom to 15 atomic planes, one plane at a time.

Graphene is a single-atom thick carbon crystal with unique properties, including superior

electrical and heat conductivity, mechanical strength and unique optical absorption.

One limiting factor in previous studies was the inability to test metal films of thicknesses below eight atomic layers.

"The key here is that unlike in metal or semiconductor films, the thickness of the graphene multilayers can be continuously and uniformly varied all the way down to a single atomic layer of graphene – the ultimate "surface" of the film," said Balandin. "Thus, we were able to accomplish with multilayer graphene films something that researchers could not do with metal films in the last century. We probed the origin of 1/f noise directly."

"We found that 1/f noise becomes dominated by the volume noise when the thickness exceeds ~7 atomic

layers (~2.5 nm)," he added. "The 1/f noise is the surface phenomenon below this thickness."

He also noted that the study was essential for the proposed applications of graphene in analog circuits, communications and sensors. This is because all these applications require acceptably low levels of 1/f noise, which contributes to the phase noise of communication systems and limits sensor sensitivity and selectivity.

"Apart from the fundamental science, the reported results are important for continuing the downscaling of conventional electronic devices. Current technology is already at the level when many devices become essentially the surfaces. In this sense, the finding goes beyond the graphene field," said Balandin.

AN OLD BASS GUITAR MADE NEW

MOUSER AUDIO APPLICATIONS SITE INSPIRES GUITAR AUDIO REVAMP

By Michael DuFault, Web Content Graphic Designer, Mouser Electronics

I recently revamped an old bass guitar after growing tired of waiting to upgrade to a new guitar. Being thrifty, I decided first to see what life I could breathe back into this cheap instrument before committing to a newer, more expensive guitar. This included completely stripping the paint, sanding out all dents and dings, refinishing with tung oil, and most importantly, totally overhauling the pickups and electronics.

As a member of the Mouser Electronics marketing team, I had recently had the opportunity to help create an audio applications site, which included a section for guitar/bass wiring. During the process of creating that site, ideas started floating around in my head about what I could do to the abused old bass I had sitting at home. Once the site was nearly finished, I made the decision to order a pack of Bourns Model 95 potentiometers, some Cornell Dubilier Orange Drop capacitors, a Neutrik input jack, some hookup wire, and some after-market bass pickups.

Using the wiring diagram on our site as a starting point, I gutted and removed the existing electronics and got to work. My bass would still be using passive pickups in a PJ configuration, volume knobs for each pickup, and a tone control knob. I installed my new pickups along with the Bourns potentiometers.

These Model 95 potentiometers have a sealed plastic housing instead of a more traditional metal housing. The pots use a sealed conductive polymer conductor rather than the typical carbon resistive element. This means they are not affected by humidity and temperature in the same way other pots are, giving the player a more consistent performance and the parts a longer life. Products in this series are also available with an audio taper, which allows a smoother transition from minimum to maximum volume and tone.

Traditionally, pots with a metal enclosure would have you ground your wiring to the back of the enclosure, but since the Model 95 uses a plastic enclosure they provide a more preferable option. Each part includes a special solder lug washer that attaches to the shaft and offers a lead to solder a jumper wire to. Using the provided washer when installing these proved to be very easy and ended up making for a far neater soldering job when all was said and done. I found that the pots themselves feel great to the touch and have a nice and extremely even taper.

Next I attached the Cornell Dubilier Orange Drop capacitor to the tone knob. After quickly soldering and heat shrinking the leads to my



solder lug and pin, I was done. The Orange Drop I used was a 100V (the lowest available and more than ample for this application) at a value of 4700 pF. My tone knob was transformed! Previously, rolling down the tone created a quickly unusable muffled mess. With the combination of the Bourns and Cornell Dubilier parts I now had a smooth taper from a full-bodied sound to a smooth and creamy, totally usable sound at the opposite end.

The last task was to replace the old input jack with a Neutrik connector. This is a pretty straightforward change but is an improvement in terms of durability. I simply fed the new long-threaded connector through the existing hole in the body and wired it up appropriately.

The cosmetic changes to the bass were by far the most difficult to do, so afterwards the wiring changes were a joy. Once I put everything back together and gave the guitar a setup, this bass played like a dream. I would now put this instrument up against basses that cost two or three times as much in a shop and no longer feel the need to trade up, not to mention that I was able to give it a personal flair that suits my playing style!

Mouser has the newest products for latest video and audio processing designs.

Mouser caters to design engineers and buyers by delivering What's Next in advanced technologies, offers customers 19 global support locations, and stocks the world's widest selection of electronic components for the newest design projects. Our website is updated daily and searches more than 10 million products to locate over 3 million orderable part numbers available for easy online purchase, and also houses an industry-first interactive catalog, data sheets, supplier-specific reference designs, application notes, technical design information, and engineering tools.

Michael DuFault is a Web Content Graphic Designer for Mouser Electronics, Inc. and a lifelong musician. He plays guitar and keyboard in Automorrow and makes chiptune music on old video game consoles as MicroD.

Mouser Electronics

Artisan Building, Suite C, First Floor

Hillbottom Road, High Wycombe

Buckinghamshire, HP12 4HJ

01494-467490

uk@mouser.com

uk.mouser.com





uk.mouser.com

The Newest Products for Your Newest Designs®

The Next Big Thing Is Here.

NEWEST PRODUCTS



More New Products
More New Technologies
More Added Every Day

Authorized distributor of semiconductors
and electronic components for design engineers.



MOUSER
ELECTRONICS



The Vital 40 Minutes

MYK DORMER IS A SENIOR RF DESIGN ENGINEER AT RADIOMETRIX LTD
WWW.RADIOMETRIX.COM

M

uch has been written recently about management theory, the correct ways to utilise “teams” of employees and how to oversee complex projects. All such work has, however, been written from the manager’s viewpoint and under the assumption that “success” is the desired outcome.

From my experience – as an engineer and an employee – I feel it is time to present the view from the bench, rather than the boardroom, and challenge that basic assumption.

Over the decades, the parade of critics, incompetents and fumblers I have reported to has convinced me that the fundamental aim of any project manager is to delay, obfuscate and misdirect available resources in order to indefinitely prolong that state of “incipient failure” which most engineering projects fall into.

That said it is probably useful to examine the management techniques available to “optimise” staff productivity. To begin with, there are certain traditional methods:

Criticise everything. There is no need to waste time evaluating an underling’s suggestion or intended course of action; just condemn it. This keeps up an atmosphere of tension and unhappiness and, if challenged over your “negativity”, you can claim to be acting in good faith as a “devil’s advocate” (and if the subordinate has a genuinely good idea and acts on it despite you, then your company benefits and you get a second round of attacks for “insubordination” or

“wasting company time”).

Set impossible levels of workload or unachievable short deadlines. A perennial favourite, this should break even the most enthusiastic of employees, as they wreck whatever is left of their personal lives trying to meet infeasible goals. You can even look like the “good guy” by being understanding when they fail. (Also make sure that they don’t get the opportunity to take their full yearly leave allocation, and then criticise them for this, too.)

Reward nothing. Don’t waste time and

From my experience – as an engineer and an employee – I feel it is time to present the view from the bench, rather than the boardroom

money on HR departments, cost-of-living raises, performance-linked bonuses, career paths, or any of the various things that other companies use to improve staff morale. Just pretend that no-one is doing anything useful, and act accordingly. If questioned, always remind your inferiors that they are “lucky to even have jobs during this recession”, while ensuring your own lifestyle is painfully visible to them (if necessary buy another car, or go on a long, expensive holiday).

It would seem from the above that there could be no further improvements to these powerful managerial techniques, but recent research suggests that there is a

further method which can be usefully employed alongside the traditional management tools: repetitive interruption.

While it is obvious that interrupting a staff member will result in reduced productivity (proportional to the time required to service the interruption), there is a previously unnoticed effect: whenever an interruption occurs, no matter how short or trivial it may be, there is a finite amount of time lost as the worker recovers from the distraction and picks up the threads of the original job. The duration of this “recovery” time is, of course, related to both the complexity of the task and the (presumably already low) motivational level of the worker, but as a rule of thumb, recent tests have shown it to be approximately eight times the duration of the interrupting task (for typical bench-engineering activities at least).

In itself, this may seem innocuous, but the consequences are far reaching. Very few interruptions (a phone call, a simple “email demanding immediate answer”, a quick “pop-in” visit to the lab, a trivial supplementary job) will in reality take more than five minutes, while their very simplicity allows them to pass unrecorded by any time-management system. Each one, however, costs the subject forty minutes of useful work-time, and this lost time can very quickly add up.

Four such interruptions in a six-(usable) hour work-day will almost halve real productivity. Nine per day will practically stop any meaningful engineering progress entirely, at the cost of only 45 minutes of valuable managerial effort. ●



Curtiss-Wright selects XJTAG to debug and test complex PCBs

“Curtiss-Wright Controls Embedded Computing, a leading designer and manufacturer of commercial-off-the-shelf (COTS) systems and board level products, is using the XJTAG boundary scan development system to improve the process of debugging and testing its range of radar, video and graphics products.”

Curtiss-Wright's video and graphics group designs rugged and benign solutions for customers across the defence, aerospace, commercial and industrial marketplaces. Its expertise encompasses radar pre-processing, scan conversion, tracking and display integrated with TV video, infra-red and sonar, as well as compression, decompression and distribution of radar and TV video across wide and local area networks.

The group's products and solutions are used throughout the world in vehicle, airborne and shipborne command and control consoles, vessel tracking, air traffic control and air defence systems. Customers include, among others, BAE Systems, Boeing, DRS Technologies, EDO Corporation, Lockheed Martin, Northrop Grumman and Raytheon.

Faced with the challenge of improving the process of debugging and testing its latest range of highly complex ball grid array (BGA) populated printed circuit boards, engineers at Curtiss-Wright's video and graphics group in Letchworth, England, set out to find a cost-effective boundary scan solution.

“We selected the XJTAG system due to its price, the speed and accuracy of fault diagnosis, and because the re-usable test scripts can be ported from project to project and migrate through design, prototyping to production and beyond,” said Alan McCormick, managing director of Curtiss-Wright's video and graphics group.

XJTAG is now being used to debug and test products such as

Curtiss-Wright's Sabre imaging platform, which combines a high-performance PowerPC processor with a multi-head, multi-layer graphics video and radar display capability in a single VME slot. It is also being utilised on the Osiris dual-channel radar interface board.

“Using XJTAG, we are able to very quickly debug and test both the boundary scan and cluster devices on our Sabre and Osiris boards, many of which are inaccessible to traditional

test methods such as flying probes, logic analysers, oscilloscopes and X-ray systems,” added Stuart Allen, senior hardware engineer at Curtiss-Wright's video and graphics group.

XJTAG enables engineers to test a high proportion of the circuit including BGA and chip scale packages, such as SDRAMs, Ethernet controllers, video interfaces, Flash memories, FPGAs and microprocessors. The ability to test both boundary scan and cluster devices gives engineers valuable extra flexibility to design tests for critical parts of the board.

“We are using FPGAs on many of our cards and with the XJTAG circuit visualisation tool (XJAnalyser), we can read and write to all the thousands of

device pins on an FPGA or another JTAG-enabled device and validate that every pin is functioning whether or not it is being utilised in the first release of the product or not,” added Stuart Allen, “this capability is very valuable.”

The XJTAG development system is a cost-effective solution for debugging, testing and programming electronic printed circuits boards and systems throughout the product lifecycle. The XJTAG system reduces the time and cost of board development and prototyping by allowing early test development, early design validation of CAD netlists, fast generation of highly functional tests and test re-use across circuits using the same devices.

opinion

Alan McCormick
managing director
Curtiss-Wright
Video and graphics group

“We selected the XJTAG boundary scan development system due to its price, the speed and accuracy of fault diagnosis, and because the re-usable device-centric test scripts can be ported from project to project and migrate through design, prototyping to production and through into field test roles. Using XJTAG, we can very quickly debug and test both the boundary scan and cluster devices on our boards, many of which are inaccessible to traditional test methods such as flying probes, logic analysers, oscilloscopes and X-ray systems.”

Data Bank	CURTISS WRIGHT Controls Embedded Computing
Company	Curtiss-Wright Controls Embedded Computing (Video and graphics group)
Nature of business	Designer and manufacturer of rugged and benign radar, video and graphics products
Main product	Products provide radar pre-processing, scan conversion, tracking and display integrated with TV video, infra-red and sonar
Customers	Defence, aerospace, commercial and industrial system integrators
Location	Letchworth, UK. Group sites in the USA, Canada and Europe
Web site	www.cwembedded.com

THE FUTURE OF FIELD PROGRAMMABLE GATE ARRAYS – THE BEST IS YET TO COME

ALTERA CELEBRATES 30 YEARS OF SUCCESS IN FPGA INNOVATION AND DEVELOPMENT THIS YEAR. ITS CTO **MISHA BURICH** ASSESSES WHAT'S IN STORE FOR FPGA CHIP TECHNOLOGY NEXT

It's a current question: Where can FPGA technology take us next?

To a first approximation Moore's Law will serve, as it has for a generation now, as the basic route map. Just putting ruler to graph-paper then suggests that in ten years we could have 5nm semiconductor manufacturing processes, which would allow for 100 billion transistors on a single die. With so many transistors, the process of silicon convergence will continue to create large heterogeneous chips, and regardless of what they might look like, they will have to offer high levels of programmability and re-configurability.

The FPGA programmable fabric will be the main driver and differentiator for such silicon-converged products, working in combination with other silicon architectures. Today we already see specific applications in which programmable fabric accelerates traditional software-executing hardware blocks, including CPUs and DSPs with the FPGA-based datapath- and instruction-decoding extensions. Programmable graphics engines, programmable video codecs, programmable compression-decompression engines for video and data, programmable encryption-decryption engines for security services, programmable network and packet processing engines, and programmable

Mischa Burich, CTO,
Altera Corp



hardware assist for the operating system services, all can benefit from FPGA-fabric assistance. These chips also tend to have lots of sophisticated cache memories in order to balance the on-chip-off-chip memory traffic. Increasingly, in order to manage traffic on such complex devices, we are seeing designers turn to programmable network-on-chip technology, including packet routers and switches.

Surprisingly, the addition of programmable fabric brings not only flexibility, but performance increases and power savings to the overall system. Because of the hardware

Because of the hardware programmability, the FPGA fabric is now more power efficient and less costly, as measured by OPS/mW, relative to the pure processor architectures

programmability, the FPGA fabric is now more power efficient and less costly, as measured by OPS/mW, relative to the pure processor architectures. As designs implemented in the fabric can employ extensive parallelism, the FPGA fabric delivers better performance for many applications relative to the processor architectures. There is no other architecture that can do a better job in

providing the solutions that meet customer performance, power and cost requirements than the silicon converged products with embedded FPGA fabric.

These silicon-converged products are either standard products or application specific standard products (ASSPs). We are seeing the early adopters for this converged architectural approach in "software-defined" solutions, such as software-defined radios and software-defined networking.

Design Constraints

More and Differentiated Features

High Performance

Lower Power

Lower System Cost

In Less Development Time

Figure 1: Chip design constraints

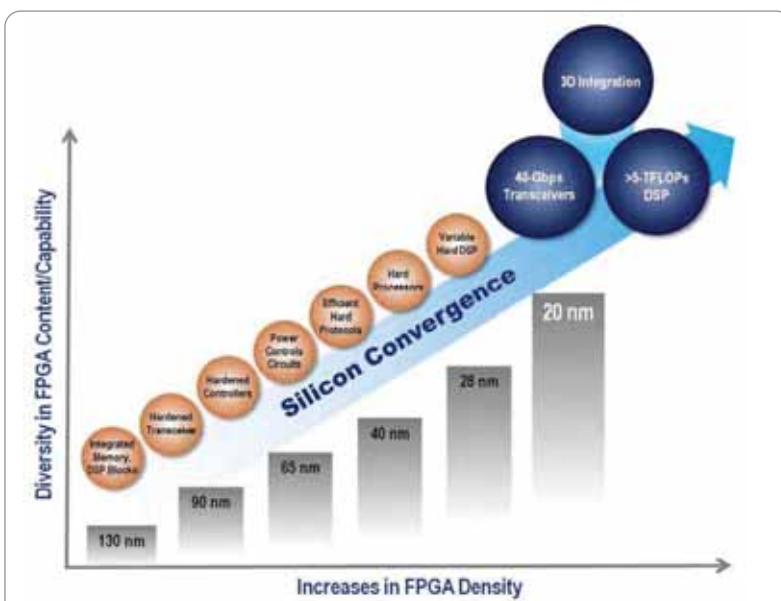


Figure 2: FPGA development with greater silicon integration

In these applications, software defines the function of the chip, but software must depend on hardware acceleration to meet the performance and power requirements of the system. These changes will sweep through the architectures of large SoCs, and software design will see a shift just as great as the architectural design.

The next generation of programmers are far more comfortable with the idea of functions that can be dynamically relocated, and this change to the current order will accelerate. Our veteran hardware design languages – and programming languages – will be superseded as new techniques are invented to speed coding and to close the gap between software and hardware. The programming model is based on a new generation of standardized parallel languages.

We are already witnessing these changes, as the coming generation of data centres will include dense clusters of

server-class CPU chips, supported by extremely large and fast FPGAs. These FPGAs will sit on the super-speed local networks along with the CPUs and shared caches, acting as virtualised, dynamically-reconfigurable network packet engines and computational accelerators.

The future for FPGAs is extremely positive. FPGAs are increasingly relevant in a world where chips must become more complex and flexible in their architectures so they can meet the needs of the markets they serve. ●

Strategies in Light Europe

19-21 November 2013 M.O.C. Event Centre, Munich, Germany www.sileurope.com

DEVELOPING THE NEW ECOSYSTEM OF LIGHTING

WHY YOU SHOULD ATTEND

- Investor Forum organised in association with Berenberg Bank, will discuss issues such as the pace of adoption of LEDs in lighting, the longer-term growth potential of the market, and opportunities to invest in different levels of the lighting value-chain
- Largest conference and trade show in Europe focused exclusively on LED lighting applications and technology
- Delegates, exhibitors and conference topics represent the entire LED lighting value chain, from components to systems
- Conference topics and speakers address issues of greatest interest to the European LED lighting community
- The only European LED conference that provides parallel tracks on markets and technology, as well as workshops and an Investor Forum
- Ample networking opportunities to meet and interact with colleagues from throughout the European LED lighting industry

For more information visit: www.sileurope.com

Owned and Produced by:



Presented by:



Supported by:



Events:



TRAVELLING AT THE SPEED OF LIGHT

MALCOLM DAVIDSON, SYSTEM AND SOFTWARE QUALITY ASSURANCE CONSULTANT TO THE OFFSHORE OIL INDUSTRY, CHALLENGES CONVENTIONAL WISDOM OF WAVE PROPAGATION, WHICH HE CALLS "THE 100-YEAR MISUNDERSTANDING"

Physicists and engineers pride themselves on developing equations and models which they perceive are an accurate representation of reality and the physical world. While these equations will be logically consistent with the paradigm they were developed in, mapping them to the physical world can indicate flaws with the model itself.

In an ideal world research builds on prior knowledge and refines the models and understanding accordingly. Sometimes however, equations and models become stuck in the past and, despite new understanding, retain their place in the pantheon of science and academia. Maxwell's equations are one such example.

Questioning the Established Wisdom

It is well known – and accepted – by physicists and electronic engineers alike that all electrical energy travels at the speed of light for the medium it is in. In vacuum or air this would be 3×10^8 m/s. Therefore, whether the signal is a sine wave, a complex wave or a step function, the energy will always be moving at the defined speed of light.

This article will show, by considering only the physical constraints of travelling at the speed of light, that it is impossible for any electric field or magnetic field associated with the signal to cause the other. Maxwell's equations require faster than the speed of light travel if the conventional interpretation is valid.

Consider a sine wave in Figure 1. This signal is propagating in the medium at the speed of light. The medium could be a twisted pair cable, coaxial cable or air. Each part of this signal is moving at the same speed, and the speed of light is defined as $c = 1/\sqrt{\epsilon_0\mu_0}$.

If we focus on a minute "sliver" of this propagating signal, the

medium and signal will be identical for any other part of the propagating wave. The fact that the original signal was a sine wave is irrelevant, for each part of the moving energy knows nothing about any other part of the signal. It only knows about itself, and it only knows about now. We may consider this sine wave signal as consisting of an infinite number of slivers adjacent to each other, all with a slightly different amplitude. Analyze a single element and the complete waveform will behave the same way. A sliver is shown in Figure 2. The sine wave is made up of "slivers" of differing amplitudes which repeat in a periodic manner, as seen by an observer, whereas a step function would be made up of "slivers" all with the same amplitude, as seen in Figure 3.

The sample signal has two properties associated with it, namely an E field and an H field, in a ratio defined by the characteristic impedance for the space travelling:

$$Z_0 = \frac{E}{H} = \mu_0 \epsilon_0 = \sqrt{\frac{\mu_0}{\epsilon_0}}$$

This fundamental electrical energy flow is commonly known as the Poynting Vector with the E and H fields at right angles to the direction of flow. It has been shown that a single potential measured in an open circuit, or a fully charged capacitor with steady state voltage (no magnetic field) has the same energy flow moving in opposite directions, hence cancelling out the H field.

As the energy moves through the medium, each segment of the signal knows only about itself, for it is travelling at the speed of light. There can be no 'a priori' knowledge about what is, either ahead of it, or what is behind it. If there were information it would have to travel faster than the speed of light, which has been shown to be impossible.

Each part of a signal is just moving through a medium. If it is a step, then all values of E, the electric field and H the magnetic field will be identical after the initial transition. As mentioned earlier, there is no knowledge inherent within the signal of what it is composed of, however an observer may 'see' it as a step function, a pulse or a sine wave. Each of these observations will be taken at one point in time as the signal passes by.

The key awareness to take away from this is that there is only a "Now" for energy; in any

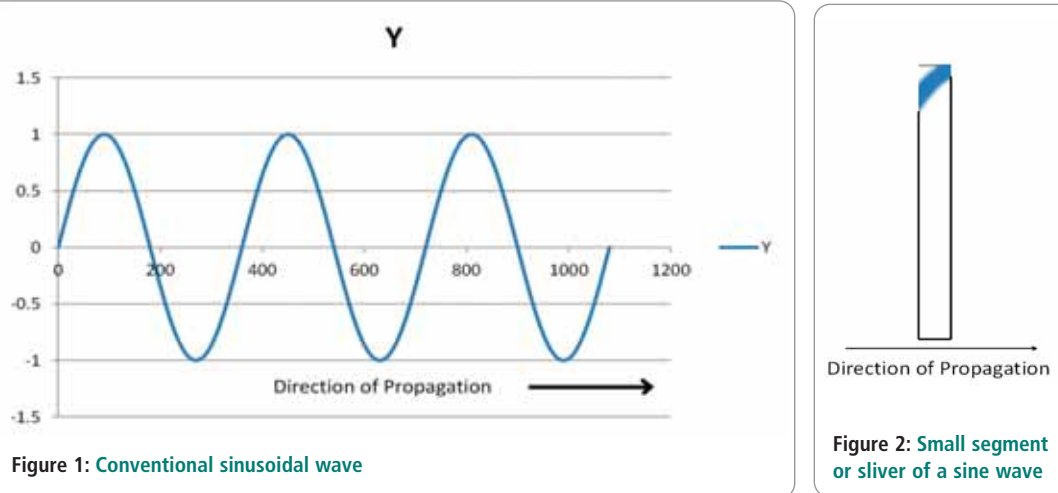


Figure 1: Conventional sinusoidal wave

Figure 2: Small segment or sliver of a sine wave

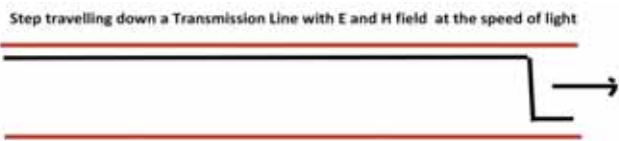


Figure 3: A digital step, typical of any binary signal

instant there is no causality within the signal itself, merely a constant relationship between the E and H components.

This concept will now be considered when we look at some of the most fundamental and key equations developed more than 100 years ago.

Basic Equations Considered

Maxwell's equations, in their differential form can be expressed as:

$$\nabla \cdot E = Q$$

$$\nabla \cdot B = 0$$

$$\nabla \times E + \frac{\partial B}{\partial t} = 0$$

$$\nabla \times B = J + \frac{\partial E}{\partial t}$$

Let's consider there can be no causality within a signal of any kind. Each equation will be reviewed from the perspective of this "sliver" of energy, having an E & H field moving at the speed of light for the medium. (We assume a constant Z_0 , which is the characteristic impedance that will result in a constant non-varying speed and, hence, no internal discontinuities.)

The electric field is:

$$\nabla \cdot E = Q$$

otherwise known as Gauss's Law: "Gauss's Law for the electric field states that the electric flux through any closed surface is proportional to the amount of electric charge contained within that surface."

The sliver can be viewed as a single location in space. We reverse the definition and state that: "The charge measured at any point in space is equal to the total electric field observed at that location".

The magnetic field is:

$$\nabla \cdot B = 0$$

otherwise known as Gauss's Magnetism Law: "The flux of the B field through a closed surface is zero".

There is no such thing as a magnetic monopole. The magnetic field can be seen as concentric rings at right angles to the direction of motion. If there is an H field travelling along a transmission line, then it is bounded by equal and opposite currents flowing in the guide wires. If we now look at the E and H fields moving along a transmission line they would look like those in Figure 4.

The varying electric field is:

$$\nabla \times E + \frac{\partial B}{\partial t} = 0$$

This infers that a changing electric field causes a changing magnetic field. The varying magnetic field is:

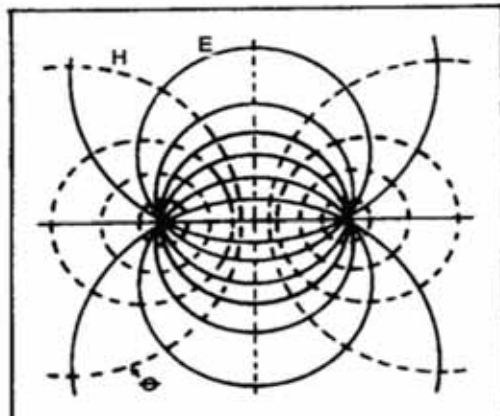


Figure 4: E and H fields are defined by the characteristic impedance of the medium

$$\nabla \times B = J + \frac{\partial E}{\partial t}$$

This also infers that a changing magnetic field causes a changing electric field. (The J term was added to cope with the observed current passing through a capacitor when the electric field was changing.)

There are many similar references to these equations stating such concepts as: "A flow of electric current will produce a magnetic field. If the current flow varies with time (as in any wave or periodic signal), the magnetic field will also give rise to an electric field. Maxwell's equations show that separated charge (positive and negative) gives rise to an electric field, and if this is varying in time as well it will give rise to a propagating electric field, further giving rise to a propagating magnetic field." [2]

Or let's consider how radio waves propagate. At the transmitter, we generate an alternating electric charge (that is an AC voltage), which we apply to a wire (the transmit antenna). A time-varying electrostatic field now surrounds the wire, in accordance with Maxwell's first equation. As the electrostatic field expands and collapses, it induces in front of it an expanding and collapsing magnetic field, the shape of which is described by Maxwell's fourth equation. This time-varying magnetic field will induce ahead of it an expanding and collapsing electrostatic field, as described by Maxwell's third equation. And so the wave propagation: expanding and collapsing electrostatic field, inducing ahead of it an expanding and collapsing magnetic field, which gives rise to an expanding and collapsing electrostatic field. Maxwell's third equation, fourth equation, third equation and so forth, until the wave reaches its destination. [3]

This is typical of many references to the physical implications of Maxwell's equations. However, when we realize that each "sliver" of any time-varying field has both an E field and an H field component that is unchanging at that instant in time and location in space, it is impossible for a time-varying field to induce anything.

The signal propagating from an antenna contains a signal which has two components (E and H) they are related by the characteristic of free space which is $120 \times \pi$, approximately 376 ohms. The speed of this waveform in space is 3×10^8 m/s. Each slightly different amplitude of the E field has a corresponding H field.

As this signal moves through space at the speed of light each "element" knows nothing about its neighbour, for it is travelling at the speed of light; it cannot "see" ahead of itself and it cannot "know" about the past – in the same way that we only know about this moment in time, the now.

One good example of a propagating wave which does not vary in

time so a changing E and changing H do not exist and so cannot cause each other is a voltage step or pulse as used in all digital devices. The step travels along interconnections with a steady state voltage such as 5V (constant E) and there will be a corresponding current for the medium, based upon the characteristic for the medium (constant H).

Further: "This time-varying magnetic field will induce ahead of it an expanding and collapsing electrostatic field... inducing ahead of it an expanding and collapsing magnetic field which gives rise to an expanding and collapsing electric field..."

The third equation causes the fourth equation causes the third equation causes the fourth equation and so forth.

Travelling at the speed of light would make "induce ahead of it" impossible; that would require travelling faster. If it was required for the E field to change in time for a digital step to propagate then the signal would not move (maybe the leading edge and trailing edge only). We have 70-plus years of knowing that this is a false notion and the step with a steady voltage and current does travel at the speed of light for the medium.

Charging a Capacitor

Consider a step function injected into a parallel-plate capacitor via a long cable such as a coax or a twisted pair. Each component can be viewed as a transmission line with particular characteristics. We are only interested in the characteristic impedance Z_o of each. In this case:

$$Z_o = \sqrt{\frac{L}{C}}$$

The equation above shows that Z_o is the square root of inductance per unit length divided by capacitance per unit length. If C is large, then Z_o becomes small, hence the value of 0.5 ohms. This appears as nearly a short circuit to an applied voltage step, hence most of the signal is reflected back towards the source. However, a small voltage propagates along the parallel plates of the capacitor and upon reaching the end of them "sees" an open circuit. This reflects back on the incoming energy, doubling the value observed at the open-circuit end.

When this front edge reaches the discontinuity between the capacitor and the coaxial cable, there will be another reflection.

$$\text{The Reflection Coefficient} = R_l - Z_o = 75 - 0.5 = 0.986$$

$$R_l + Z_o = 75 + 0.5$$

Nearly all of the signal is reflected back into the capacitor, with a

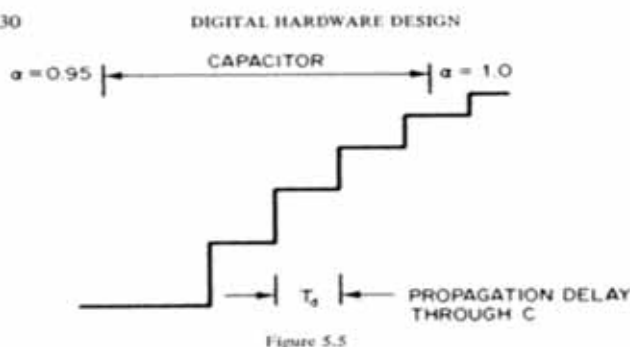


Figure 5: Flux of the electric field through a closed surface is due to the charge density enclosed

slightly smaller amplitude. After many reflections there is a balance between the energy flowing from the left and the right. Figure 5 shows the incremental build-up of charge using the distributed model. [4]

The H or magnetic field has been cancelled out finally, so there is no current flow observed. The capacitor is said to be fully charged. However, note that the energy continues to flow. The TEM wave is propagating in both directions within the capacitor. When we now apply a sinusoidal time-varying field to a capacitor, the energy propagating into the device is constantly changing, so the reflected signal will always be different to the applied signal. This is because the capacitor is distributed in space (has dimension). Subsequently, the H fields will not cancel and thus an electric current will be measured. This is known as "displacement current" and is merely the difference between the Poynting Vector signals moving in opposite direction.

We always consider the sine wave to be made up of sequential slivers of energy with differing amplitudes. Therefore, the physical concepts outlined here apply to all kinds of waves.

Process of Integrating New Information

As a society we generally believe that current theories have built upon the ideas of the past, refined them, added to them and filtered out those which no longer apply. For example, Sir William Preece, Head of the British Post Office in the early 1900s thought the correct model for a transmission line was a lumped RC model (resistance and capacitance). Oliver Heaviside argued that the model must include L, inductance. Heaviside's model was more accurate, despite many protestations to the contrary. The LCR model became part of the accepted scientific truth and integrated into conventional theories.

Now, with the advent of much faster electronic systems, we have to continue to be open to new models and more accurate equations for non-lumped components. The reliable functioning of these devices relies upon appropriate equations and models.

How does industry, or indeed academia deal with change, cope with modifying their world view in light of new information, new demands of reality? Ultimately, as physicists, scientists or engineers we must seek the truth. Why be an instrumentalist and settle for conventional wisdom? As physicists are pushing the boundaries of knowledge daily in the pursuit of the origins of the universe, we must do likewise within the domain of electrical energy propagation.

Any equation or model which requires a mindset which disobeys one of the basic laws of nature, by definition, cannot be accurate, regardless of its history or perceived importance. The process of acquiring and integrating new information may demand that we close one door on a widely accepted model, but this will afford us the opportunity to open up another door. With courage we can step into this new world and forge new equations and new models which adhere to the natural world and not to the dusty tomes of the past. ●

REFERENCES

- [1] Maxwell's differential equations simplified for waves in free space. See reference:
<http://www.setileague.org/articles/ham/maxwell.pdf>
- [2] <http://maxwells-equations.com/index.php>
- [3] "Maxwell without Tears" by H. Paul Shuch Penn College of Technology.
<http://www.setileague.org/articles/ham/maxwell.pdf>
- [4] Reference: Digital Hardware Design Catt Walton Davidson 1979 Macmillan Press

RFI/EMI shielding gaskets & components

Kemtron
Proven EMC Shielding Performance
www.kemtron.co.uk
+44 (0) 1376 348115 · info@kemtron.co.uk



SDR Demonstrator for Wireless Data Systems

The DE9941 is a credit card sized demonstration platform for a complete Software Defined Radio (SDR) for wireless data applications. It is designed to be small and low-cost with minimal components/values.

The board integrates CML's market-leading RF devices:

- CMX998 Cartesian Loop Transmitter
- CMX994 Direct Conversion Receiver
- CMX7164 Multi-mode Wireless Data Modem

Features and Benefits:

- Demonstration of an SDR Wireless Data Modem
- On-board PLL and VCO for 452MHz to 467MHz operation
- Only one serial interface (CBUS/SPI) required for control and data transfer
- 1W Transmitter Operation
- Nominal +3.6V Supply
- Small 83mm x 55mm size

10:1 Input dc-dc converter 240/280W

The HR series of dc-dc converters are designed for use in transportation and other advanced electronic systems. The extremely wide input range of 12Vdc to 168Vdc and configurable output provides a single unit solution for a vast range of applications. Features include high efficiency, high reliability, low output noise, and excellent dynamic response to load/line changes.

The converters are particularly suitable for railway applications operating from all common dc traction supplies: 24V, 36V, 48V, 72V, 96V, 110V & 120V nominal voltage. The converters comply with EN51055 and EN50121-3-2, IEC/EN 60950-1, IEC61000-4-2, -3, -4, -5, -6.

The output is configurable as 12Vdc, ±12Vdc or 24Vdc; LED indicators display the status of the converter. They can be plugged into a 19" rack system according to IEC60297-3, or be chassis mounted. Cooling plates are available for conduction cooled applications or heat-sinks for convection cooling.

Extremely wide input range 12 to 168Vdc
Inrush current limitation
Input overvoltage protection
Programmable undervoltage lockout
Zero load, overload & short-circuit proof
Parallel operation with current sharing
High efficiency to 94%
Very high reliability
Operating temperature range -40°C to +71°C

Relec Electronics Ltd
Tel: +44 1929 555700 Fax: +44 1929 555701
e-mail: sales@relec.co.uk

www.relec.co.uk
Design solutions for design engineers

IDEAS FOR USING A CHARGE TIME MEASUREMENT UNIT

PADMARAJA YEDAMALE FROM MICROCHIP TECHNOLOGY PRESENTS NO LESS THAN 48 APPLICATIONS OF HOW AND WHERE TO USE A CHARGE TIME MEASUREMENT UNIT (CTMU) TO TAKE ADVANTAGE OF ITS FEATURES

Since its introduction in PIC microcontrollers, the Charge Time Measurement Unit (CTMU) has become popular for creating simple and low-component touch control solutions. Some applications have used its ability to resolve the time difference between inputs down to the sub-nanosecond range. But thinking that the CTMU can only deal with time and charge measurements would be a serious underestimation of its abilities.

As proof of its versatility, here are several different applications and categories of applications that can be implemented with the CTMU. Many of these implement new functionality in existing control applications, using only a few or no additional components. These applications are basic ideas, presented in an abbreviated format that can be used as a starting point for developing your own solutions.

Charge Time Measurement Unit (CTMU)

The CTMU is an on-chip constant-current source, surrounded by digital circuitry to precisely control its operation (Figure 1). The current source operates over four decade ranges, from $0.55\mu\text{A}$ to $550\mu\text{A}$. When combined with the on-chip A/D converter and comparators, the CTMU can perform a variety of basic functions including capacitance measurement (relative and absolute), inductance measurement (relative), resistance measurement (relative and absolute) and high-resolution time measurement.

While the basic functions are useful for a variety of applications, they can also be used as the basis of more complex tasks, such as temperature measurement, current source (constant and variable), precise time delay generation and Pulse-Width Modulation (PWM) output.

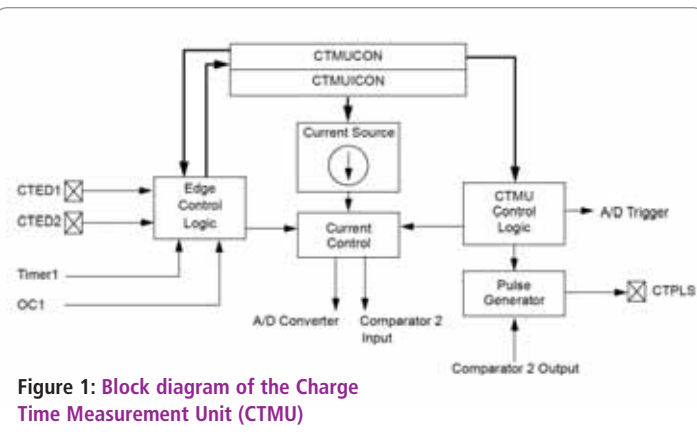


Figure 1: Block diagram of the Charge Time Measurement Unit (CTMU)

APPLICATIONS BASED ON ELECTRICAL PRINCIPLES

Relative Capacitance Measurement

By far, relative capacitance measurement is the most used principle in designing applications for the CTMU. This is not surprising, because there are numerous applications that require relative capacitance measurement. When a constant-current source is available, measuring the relative capacitance is easy. The constant-current source (I) charges the unknown external capacitor (C) to a voltage (V) in time t.

From the basic equation for capacitance, $I = C \frac{dV}{dt}$, when the current and time are constant, the voltage $V = I * t / C$ varies inversely with the capacitor value. In a relative capacitance measurement application, such as capacitive touch sensing, when a finger touches a capacitive touch pad, the capacitance increases, thus decreasing the voltage charged. As an example, take a simple touch application (shown in Figure 2) with a total capacitance – including parasitics, like the switch (CSW) and circuit (CCIR) of 30pF . When the external circuit is charged with a current of $5.5\mu\text{A}$ for $10\mu\text{s}$, this produces a voltage of 1.83V . When you add the touch of a finger, an additional capacitance (CF) of up to 10pF is added. The exact amount of capacitance depends on how much the touch pad is covered by the finger and any covering material over the pad. For a 10pF change, with the same current and charge time, the voltage is 1.38V . The voltage is measured at frequent intervals by the microcontroller's A/D converter. Changes (particularly decreases) can then be interpreted as a touch event.

All of the following applications use the same basic principle:

1. Capacitive Touch Sense Controls

As just described, relative capacitance change can be used to control an application in the same way as scanning switches, push buttons or touch screens do. By using the A/D converter's multiple input channels with the CTMU, multiple touch controls can be implemented.

2. Microphone (Direct Audio-to-Digital)

The capacitance of the microphone's element changes continuously in proportion to the frequency of the vibrations hitting its diaphragm. The microcontroller's ADC constantly samples the resulting voltage and creates a digital signal.

3. Proximity Sensor

Very often, a direct touch isn't needed to change the capacitance of a circuit: the near-by presence of a hand to a PCB may be enough. With the proper components, software tuning and layout selection, the CTMU can be used to sense proximity the exact same way as it senses touch.

4. Stud Finder

A stud on the other side of the wall (metal or not, with or without nails or metallic fasteners) will change the local capacitance of the

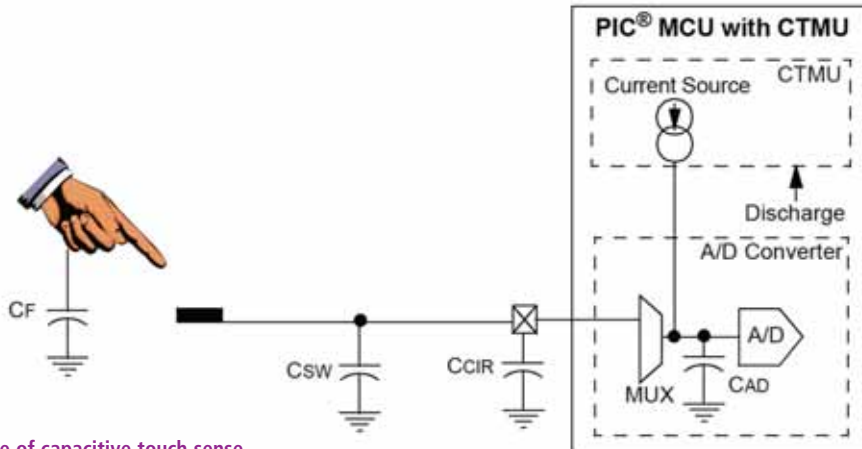


Figure 2: Basic principle of capacitive touch sense

wall's surface.

5. Occupancy Sensing

Rather than using the old, interrupted photocell principle, a capacitance sensor can be embedded in the doorway, so whenever a person passes through, the sensor's capacitance changes.

6. Liquid Level Sensing

Here is a clever twist on capacitance. Take a conductive plate and place a container made of an insulating material (say, glass) upon it. Fill the container with a liquid and you have a capacitor. In this set-up, the capacitance of the container changes with the level of the liquid. The size of the container and the plate can be scaled according to the application's requirements. (Note that the application requires calibration for each different container and each type of liquid.) Level sensing can also be implemented using a conductor running along the length or height of a container. The operating principle is exactly the same.

7. Pressure/Force Sensor

Take two conductive plates, one fixed and the other spring-mounted. Besides having an air-dielectric capacitor, you have a sensor which changes capacitance in proportion to the weight or force applied to the spring-mounted plate. This gives a variation of a strain cell and a method to directly measure pressure (and perhaps weight) with the CTMU.

8. Automatic Litter Box

Relative capacitance sensing is not just for liquids or finger touches. Cat litter, for example, can also be measured for capacitance change – when the litter is unused and when the cat has finished with it. The change in capacitance can be used to trigger a cleaning cycle.

Absolute Capacitance Measurement

Quantifying a capacitance with some measure of precision is almost as simple as measuring a relative capacitance change. There are two steps required, as shown in Figure 3. First, it is necessary to calibrate the CTMU current source. The calibration procedure is simple; using a high-precision (0.5% tolerance or better) resistor of known value and a precise voltage measurement to calculate the actual current. With this information, the current source is

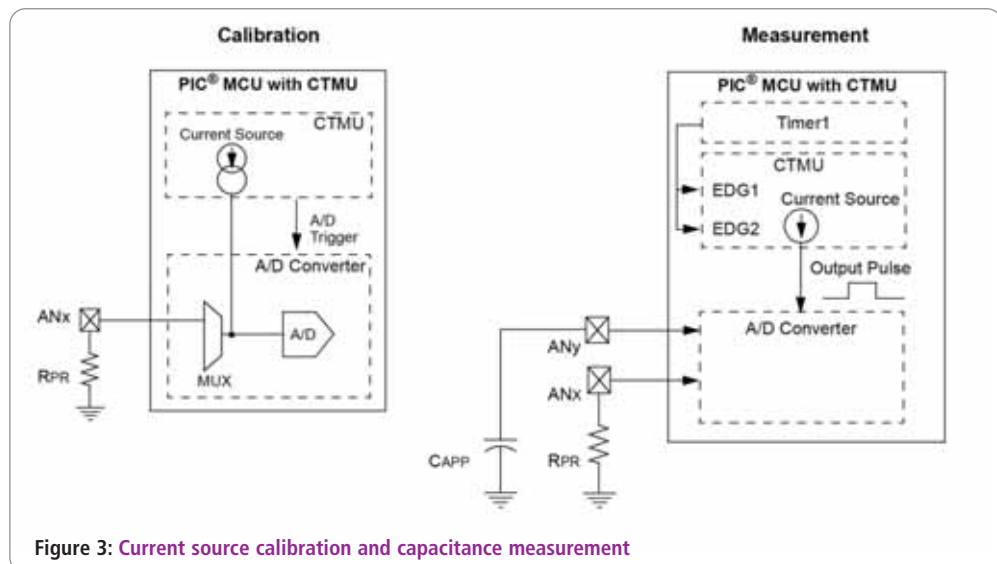


Figure 3: Current source calibration and capacitance measurement

trimmed using the appropriate control bits.

Once the current source is calibrated to the required accuracy for measurement, switch the current source to the ADC/CTMU channel where the target capacitor device is connected. The constant-current source (I) charges the unknown external capacitor (C) for time T. The capacitance is then calculated by the equation $I \times T = C \times V$, where I and T have already been defined, and V is measured by the microcontroller's ADC.

There are numerous applications that require absolute capacitance measurement. These include:

8. LCR Meter (Capacitance Function)

The CTMU can directly measure an unknown capacitor to establish its capacitance or confirm the value of a labelled, but questionable capacitor.

10. Humidity Sensing

The latest generation of precision polymer humidity sensors provides their output as a change in capacitance, rather than the more traditional voltage or current. In an absolute capacitance configuration, the CTMU and A/D can quickly turn a capacitance change into voltage and, from there, into relative humidity.

Relative Inductance Measurement

Although most often associated with capacitance and/or current, the CTMU can also be used to measure changes in inductance.

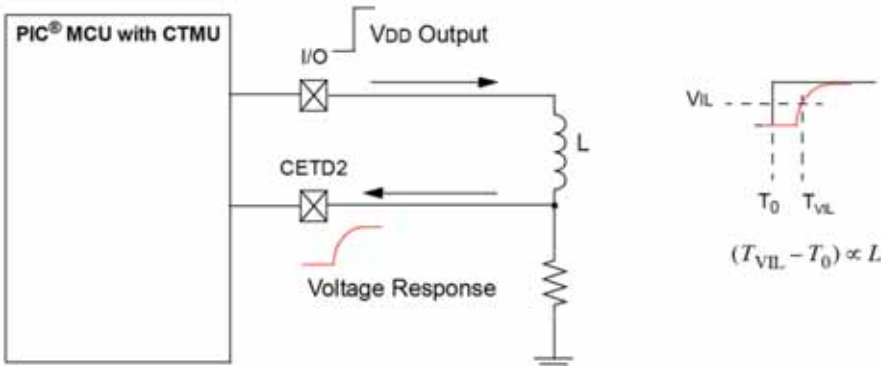


Figure 4: Measuring relative inductance change by time delay

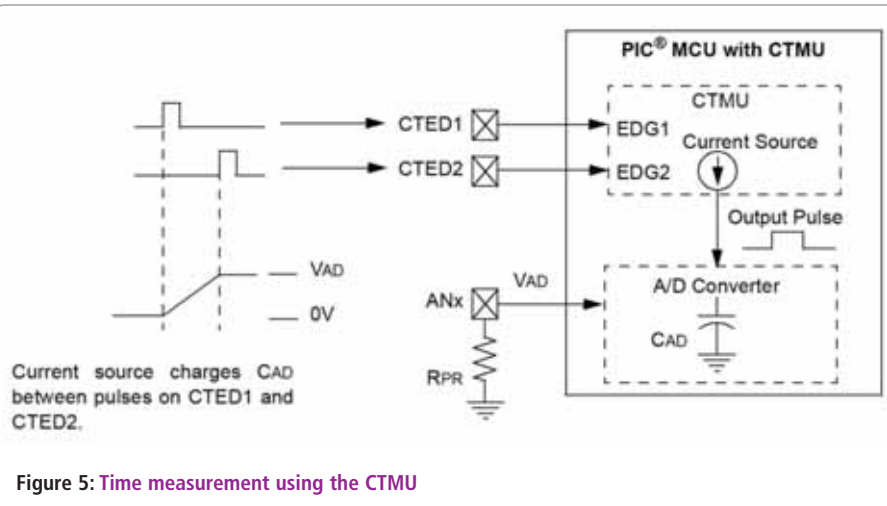


Figure 5: Time measurement using the CTMU

Strictly speaking, what is actually being measured is the inductor's time constant. A typical configuration (Figure 4) shows how this is done.

An I/O pin is set to output VDD to an inductor; at the same time, Edge 1 in the CTMU is manually set as if it had received a pulse. The voltage from the I/O pin is slightly delayed in reaching CETD2 as it saturates the inductor. The time measured between the initial pulse and when the voltage on CETD2 reaches its minimum input threshold, V_{IL} (T_{VIL}), is proportional to the inductance. The CTMU takes a continuous series of "snapshots" of the inductor's time constant and compares it to an established baseline. When the time constant changes, an event is detected. Example applications include:

11. Metering

Many of the current technology flow-meters use a piece of metal on a rotor that comes to the proximity of an inductor. The repeating change of inductance can be used to determine the rate of rotation, and thus the flow through the meter. The CTMU provides another simple method to measure this change and count events.

12. Weather Station (Wind Speed Sensor)

Similar to metering applications, the CTMU can inductively sense and count the number of revolutions per minute of an anemometer; the microcontroller translates this into wind speed. When combined with a humidity sensor and a simple diode, the CTMU can implement a single chip solution for a fully functional weather station (see applications # 10 and # 33 for more information).

13. Coin Operated Vending Machine

An inductive sensor is used to detect coins as they are inserted. The CTMU can be used to quantify the number and type of coins. It could also be used to detect (and reject) slugs, which have a different magnetic signature than coins.

14. Proximity Sensing, Part Two

All of the above applications are specific cases of the same principle. Any application that is based on inductive or magnetic proximity sensing (e.g. solenoid position) can be implemented with the CTMU as the inductor interface.

Precision Time Measurement

Numerous applications require very precise time measurement. Using the edge trigger pins (CTEDn) on the CTMU, time can be measured precisely to a resolution of under a nanosecond. This is done by charging the A/D Sample-and-Hold (S/H) capacitor between the rising edges of the two pins; the resulting voltage is directly proportional to the time. Figure 5 shows the general scheme for time measurement. CTMU-based time measurement is asynchronous to the clock running the microcontroller.

Applications include:

15. Distance Measurement (Ultrasonic and Laser Devices)

The CTMU is used to measure the round-trip return time between an initial transmitted pulse and its reflected return signal. This can determine a distance measurement, accurate

to within one foot.

16. Adaptive Cruise Control

As an extension of the last application, Adaptive Cruise Control (ACC) is the active system that maintains a constant distance between moving vehicles, based on continuous measurements. The CTMU provides an RF or laser-based ranging solution to the system.

17. Safety Braking

This is the partner of Adaptive Cruise Control; it automatically triggers the brakes when the object ahead comes too close. Even when ACC is not used, its CTMU-based ranging solution can be used just as well for an independent, safety breaking application.

18. Coaxial Cable Measurement (Length, Short or Open)

The CTMU can be used to implement a simple Time Domain Reflectometry (TDR) measurement device, used to locate an open or short defect in a coaxial cable. The location of the defect is based on the time it takes for a pulse to be reflected back (Figure 6). When a voltage pulse is injected at Node A, an open or shorted cable will reflect a pulse back at a time that is proportional to twice the distance to the defect (2 TO). A properly terminated cable will not return a reflected pulse.

19. Ultrasonic Flow Meters

Like distance measurement devices, the CTMU measures the time difference between transmitted and received pulses. In this application, however, the time difference between fixed transducers varies with the flow rate of the medium being measured.

A simple flow measurement system is shown in Figure 7. In this

set-up, the microcontroller sends a pulse for transmission by the ultrasonic transceivers, while the Input Capture and Output Compare modules receive incoming signals from the transceivers. The CTMU uses the received signals that are coupled with the flow to calculate the time difference and thus, the flow rate.

20. Global Positioning System (GPS) Signal Interface

The basis of GPS is to triangulate a position from satellites, based on signal travel time. By using the CTMU to measure the time difference between individual satellite signals, the relative position on the earth can be determined. The high precision of the CTMU's time measurements allows a position accuracy that approaches the accuracy limits of the entire satellite system.

21. Pulse Width/Duty Cycle Decoding

The CTMU can accurately measure individual pulse widths of an incoming pulse train. If data has been encoded in the stream using PWM, the CTMU can be used to demodulate the stream and restore the digital information. PWM is found in many applications, such as infrared remote controls.

22. DTMF Detection and Decoding

The same principles of decoding a width-modulated pulse-train can also be used in DTMF applications. By measuring the pulse widths of the product signal, it is possible to determine which two frequencies were used to produce it and, therefore, which key was pressed.

23. Frequency Meter

Similarly, by measuring the time between the rising edges of a signal with a constant wavelength, it becomes simple to calculate the frequency (from $f = 1/T$). This makes the CTMU a relatively inexpensive front-end for any frequency measuring application.

24. Decoder for Optical Encoders

The CTMU can read the incoming pulse trains from the (typically) three outputs of an optical decoder and determine the pulse speed and phase difference between them. This data can be translated into rotational speed and direction, and (with three inputs) absolute rotational position.

25. Optical Gyros

These devices measure changes in position by sensing the phase difference between two light beams travelling in opposite directions around a fibre-optic loop. By sensing the edges of the two signals and comparing them to the single source that created them, the CTMU can be used to calculate the phase difference and thus, any relative motion in the device.

Resistance Measurement

Ways of measuring capacitance and inductance have already been demonstrated, so why not resistance?

The CTMU's constant-current source and Ohm's law makes this easy: if it is known what the current and the voltage being provided are, or if the voltage can be measured directly, the resistance is simple to calculate. Examples include:

26. Resistive Temperature Device (RTD)

A platinum resistor, with a known temperature coefficient, is used in many applications to measure precise and high-resolution temperatures to over 1000°F. By driving the RTD with a constant-current source, the voltage read by the microcontroller's ADC varies with the

temperature. This low-component-count CTMU solution replaces an analog circuit with many discrete components.

27. PTC and NTC Sensors

Positive or negative coefficient temperature sensors (PTCs or NTCs, respectively) give an alternate way to measure temperature, up to a few hundred degrees Celsius. These thermistors are less expensive and are nonlinear with respect to temperature. Typically, NTCs and PTCs are implemented in a voltage divider format to measure temperature. Using the CTMU's constant-current source, the resistance can be measured directly and the temperature derived from the resistance.

APPLICATIONS BASED ON DERIVED PRINCIPLES

Temperature Measurement (Constant-Current Source)

In these applications, the CTMU's constant and accurate current source can be used to exploit a basic principle of semiconductors: the P-N junction's forward band-gap voltage. When a diode is driven with a constant-current source, the forward voltage (V_F) varies inversely with the temperature.

Figure 8 shows how a diode (or any convenient P-N junction) is connected to the CTMU to create temperature measurement. Using the CTMU, together with a 12-bit ADC, temperatures can be measured with a resolution of 1°F. [Additional technical details are provided in Microchip's Technical Brief, TB3016, "Using the PIC MCU CTMU for Temperature Measurement" (DS93016).]

Applications in this category include:

28. Thermometers

General-purpose thermometers can use a cheap silicon diode in place of a more expensive thermistor or dedicated sensor for temperature sensing.

29. Thermostats

The CTMU allows the microcontroller at the heart of the application to also monitor the temperature directly, all with only one additional (and inexpensive) component.

30. PCB Temperature Monitoring

In applications where boards are either potted or in an enclosure, the CTMU with a diode can add an inexpensive monitoring solution.

31. Server Temperature Monitoring

In addition to just monitoring temperature, the microcontroller can also serve as a control to one or more chassis cooling fans, providing an extra level of safety to an expensive piece of hardware.

32. RTCC/FRC Calibration

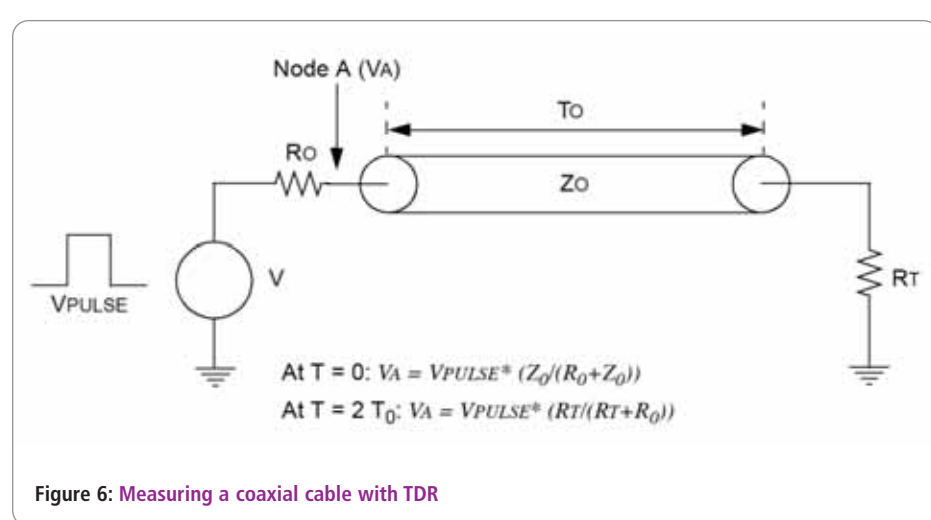


Figure 6: Measuring a coaxial cable with TDR

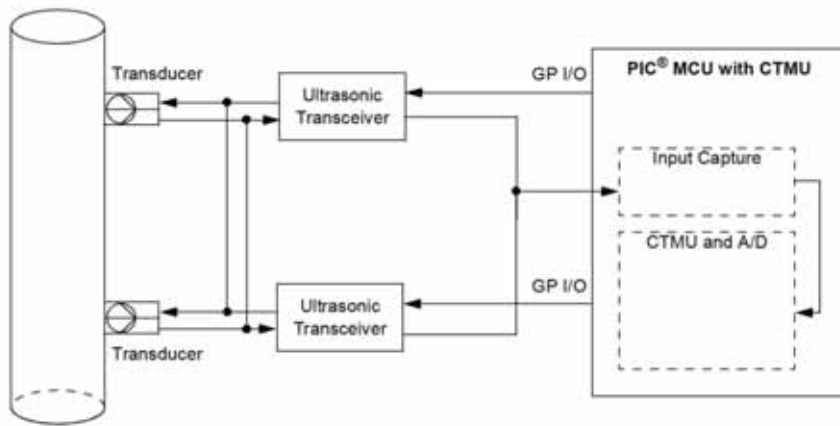


Figure 7: Ultrasonic flow measurement system

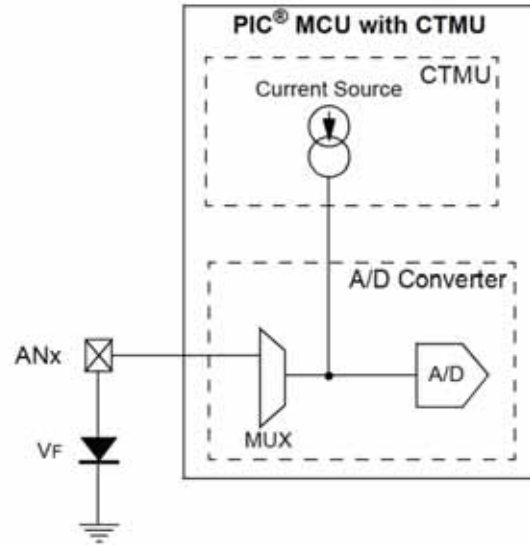


Figure 8: CTMU temperature measurement circuit

The on-chip RC oscillators on many microcontrollers may have a high temperature coefficient, with accuracy varying widely across the operating range. Using the CTMU temperature can be measured right at the application (instead of being approximated from the environment's temperature) and the oscillator's frequency trimmed appropriately.

33. Indoor Weather Monitors

Along with a humidity sensor (see # 10), the CTMU can be used to measure temperature and humidity at the same time. With a microcontroller that can drive an LCD display, this can create a single-chip solution. This application can also be the core for more complex weather stations (see # 12).

34. LED Lighting Control

In high-wattage, solid-state lighting applications, the LEDs can generate a lot of heat – perhaps not as much as an incandescent or halogen source – but enough to change the colour band reliability or the light output if temperature is not controlled.

The CTMU, along with a sensor diode, can measure temperature at the heat sink or in the environment (for forced air cooling). At the same time, another CTMU channel can actually use the LED to measure its own temperature by measuring its forward bias voltage.

This information can be used to reduce power or increase cooling when things get too hot.

35. Motor Temperature Monitoring

For electric motor applications that use a microcontroller to regulate speed and/or power, the CTMU can provide an additional control dimension: measuring the motor winding's temperature and providing thermal protection by shutting things down before the breakdown temperature is reached.

36. Assorted Home Applications

There are many electronic applications around the house that require temperature sensing or that could benefit from it. If the application requires a microcontroller, the

CTMU provides an easy way to implement temperature sensing. Examples include:

- Refrigerators
- Free-standing freezers
- Coffee makers
- Room air-conditioners
- Dehumidifiers
- Space heaters
- Climate controlled storage (e.g. wine chillers)

37. Assorted Automotive Applications

By the same principle the list can be expanded to include cars. Any system that requires temperature monitoring can use the CTMU as a solution. Cabin climate control (single and multi-zone) and engine temperature monitoring are just two examples.

Variable Current Source

38. Current Loop Control Applications

Industrial process control instruments often use current loop communications to provide noise immunity. For systems operating in the 4-20mA range, the CTMU's current source can be used with an external current mirror circuit to create a variable current control transmitter.

PWM Generation

By using the CTMU with a comparator (either internal or external), there is a way to generate high-resolution, high-frequency Pulse Width Modulation (Figure 9). The PWM resolution depends on the slope controlled by the internal A/D sampling capacitor (CHOLD) and can be changed by adding an external capacitor parallel to CHOLD.

39. Blanking Pulse for Radar

Modern radar generates transmit pulses at a very high rate and requires very high-speed display blanking to keep the receiver and display from being overwhelmed. Often, the switching rate is too fast for a conventional PWM generator. When working as a pulse generator, however, the CTMU can operate fast enough to keep up.

Digital-to-Analog Conversion

By taking PWM generation an additional step, running the high-frequency pulse output through a low-pass filter creates an analog signal. This can be useful in a number of applications:

40. Audio Generator

In a digital world, this is always a popular application: turning a digital bitstream into audio. In appliances where a microcontroller

is already present, the CTMU can implement a simple audio generator to create a range of audio feedback prompts (constant or interrupted tones of various frequencies). With enough memory, the CTMU DAC can even reproduce voice samples.

41. Digital LCD Contrast Control

For backlit displays, the CTMU can translate digital control inputs into a control voltage for changing the contrast of an LCD panel.

42. Programmable Voltage Reference

Similar to the preceding application, the CTMU DAC can be configured to generate a known voltage output for a given digital input. This can be used as the constant voltage source for many analog and control applications.

Time Delay Applications

43. Silicon Tester

The CTMU's pulse delay feature makes it easy to create a variable clock delay generator. This can be used for performing Sample-and-Hold sweeps on digital circuits as part of the validation and characterization process.

44. Oscilloscope Enhancement

For slow and inexpensive oscilloscopes, a CTMU-based solution can be used to enhance the input measurement resolution. This uses the pulse delay feature to add delayed triggers to sample the ADC for repetitive waveforms. The time delay works as multiple triggers for the A/D to acquire samples derived from a single trigger, with delays added.

45. Time Domain (Delay) Encryption/Decryption

A novel way to encrypt a digital data stream is to add fixed delays of one or more durations to the pulse train. Without knowing where the delays were inserted, it becomes impossible to establish a reference frame to decode the signal. But where the delays are known, the CTMU's pulse delay function can be used to effectively remove the delays and restore the pulse train to its original form.

The pulse delay feature can also be used to perform the initial encryption. A simplified version of the process is shown in Figure 10. Of course, this involves more than just the CTMU hardware, such as determining a key sequence and frame sync; but the point here is the decoding hardware does not need to be the difficult or expensive piece of the application.

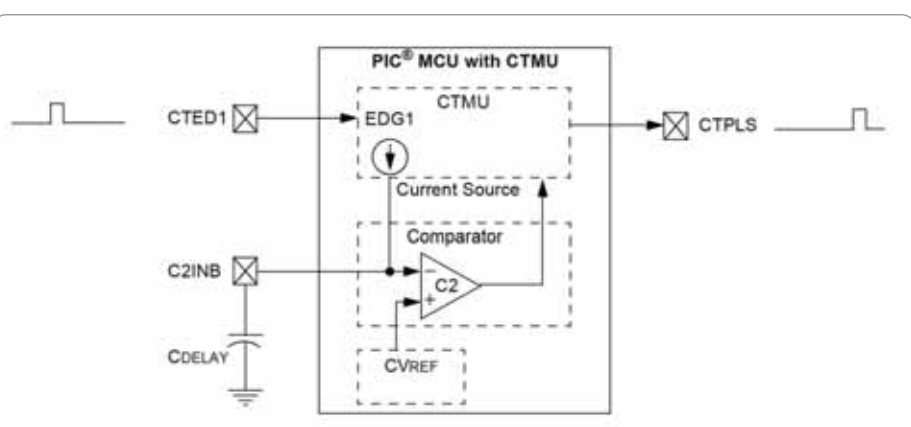


Figure 9: PWM and pulse generation

Medical Applications

46. Ultrasound Imaging (Sensor Head)

As described in previous applications, the CTMU can be used to measure the time between transmitted and reflected impulses. This information can be continuously fed in real time to a graphic processor or processing application to create an image. This can be implemented directly as an ultrasonic microphone (# 2) or indirectly, through an ultrasonic pick-up (# 15).

Really Complex Applications

47. Solving World Hunger

By mass deploying inexpensive temperature (# 28) and humidity sensors (# 10), it becomes possible to make continuous, fine resolution measurements of climatic variation over large agricultural areas. This makes it possible, at least in theory, to create a closed-loop system of more precise water and nutrient delivery. This in turn can push crop yields to their maximum. Do this in enough places and there will be enough food to feed everyone, everywhere.

48. Bring About World Peace

Admittedly, world peace is still being worked on. It's possible that it is beyond the scope of the CTMU, or it could be that it hasn't been given enough time. Perhaps this is one issue can be left to the reader.

At first glance, a constant-current source on a microcontroller might seem to have limited possibilities. What has been shown is that the CTMU, combined with the many other peripherals available in PIC microcontrollers, offers a simple way to create a wide range of applications. The 48 examples shown here just scratch the surface of what is possible. The reader is invited to expand the possibilities. ●

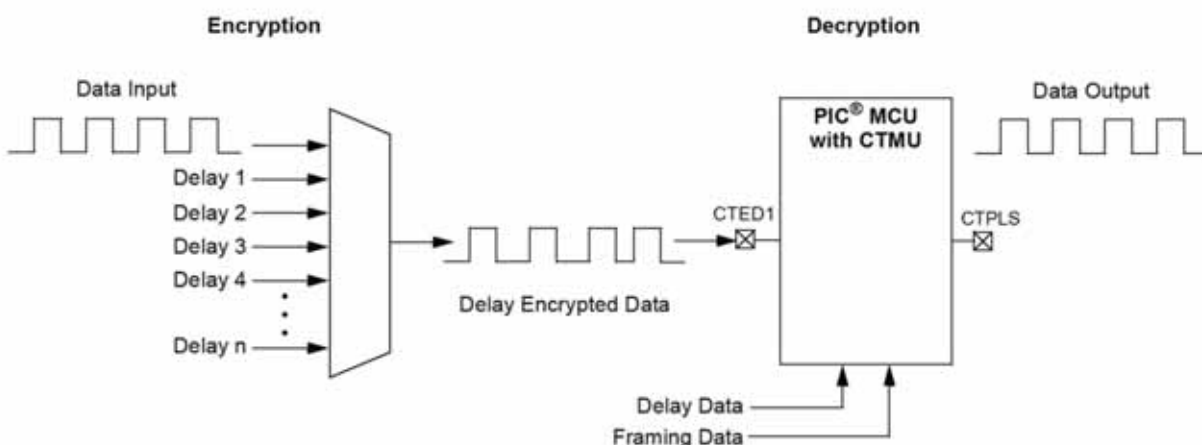


Figure 10: Simplified flow for delay encryption/decryption

ACCURATELY PREDICTING PLL REFERENCE SPUR LEVELS DUE TO LEAKAGE CURRENT

MICHEL AZARIAN, SENIOR APPLICATIONS ENGINEER, AND **WILL EZEL**, DESIGN SECTION LEAD FOR MIXED SIGNAL PRODUCTS AT LINEAR TECHNOLOGY PRESENT A SIMPLE MODEL FOR ACCURATELY PREDICTING THE LEVEL OF REFERENCE SPURS DUE TO CHARGE PUMP AND/OR OP-AMP LEAKAGE CURRENT IN PLL SYSTEMS



The phase locked loop (PLL) is a negative feedback system that locks the phase and frequency of a higher frequency device – usually a voltage controlled oscillator (VCO), whose phase and frequency are not very stable over temperature and time – to a more stable and lower frequency device, usually a temperature compensated (TCXO) or oven controlled crystal oscillator (OCXO).

As a black box, the PLL can be viewed as a frequency multiplier. It is employed when there is a need for a high frequency local oscillator (LO) source. There are many example applications, including wireless communications, medical devices and instrumentation.

Figure 1 shows the building blocks of a PLL system used for generating an LO signal. The PLL integrated circuit (IC) usually contains all clock dividers (R and N), phase/frequency detector (PFD) and the charge pump, represented by the two current sources, ICP_UP and ICP_DN.

The VCO output is compared to the reference clock, in this case the OCXO output, after both signals are divided down in frequency by their respective integer dividers N and R, respectively. The PFD block controls the charge pump to sink or source current pulses at the f_{PFD} rate into the loop filter to adjust the voltage on the tuning port of the VCO (V_{Tune}) until the outputs of the clock dividers are equal in frequency and are in phase. When they are equal, it is said that the PLL is locked.

The LO frequency is related to the reference frequency, f_{REF} , by the following equation:

$$f_{LO} = \frac{N}{R} \cdot f_{REF}.$$

The PLL shown in Figure 1 is called an integer-N PLL because the feedback divider (the N-divider) can only assume integer values. When this divider assumes both integer and non-integer values the loop is called a fractional-N PLL.

Here we will focus only on the integer-N PLLs, as different mechanisms are at work in fractional-N PLL.

Integer-N PLL Non-Idealities

The PLL IC contributes its own non-idealities to the system, principally phase noise and spurious.

The PLL system of Figure 1 acts as a low-pass filter on the reference clock phase noise and as a high-pass filter on that of the VCO. The low-pass and high-pass filter cutoff frequency is defined by the loop bandwidth (LBW) of the PLL. Ideally, the LO phase noise follows that of the reference clock converted to the LO frequency (that is, multiplied by N/R) up to the LBW and subsequently follows the phase noise of the VCO. The PLL IC's noise contribution elevates the phase noise in the transition area.

Figure 2 is a phase noise plot generated by PLLWizard, free PLL design and simulation tool from Linear Technology. The figure shows both, the total output phase noise ("Total") and the individual noises at the output due to the reference ("Ref @ RF") and the VCO ("VCO @ RF"). The IC's noise contribution can easily be seen in the circled area in Figure 2.

Any unwanted signal on the power supplies shown in Figure 1 (V_{OCXO} , V_{CP} and V_{VCO}) can translate into a spurious signal (spurs) on the LO signal. Careful design of these supplies greatly reduces or even eliminates these spurs. Charge pump related spurs are, however, inevitable. But, they can be reduced with careful PLL system design.

These spurs are commonly referred to as reference spurs, though reference here does not mean the reference clock frequency, but it refers to f_{PFD} . An LO signal produced by an integer-N PLL has dual sideband spurs at f_{PFD} and its harmonics.

Figure 3 shows the spectrum of a 2.1GHz LO signal. Here, f_{PFD} is 1MHz ($N = 2100$) and the reference clock is 10MHz ($R = 10$). The loop bandwidth is 40kHz.

Causes of Reference Spurs

In steady-state operation the PLL is locked and, theoretically, there is no longer a need to engage the ICP_UP and ICP_DN current sources of Figure 1 during every PFD

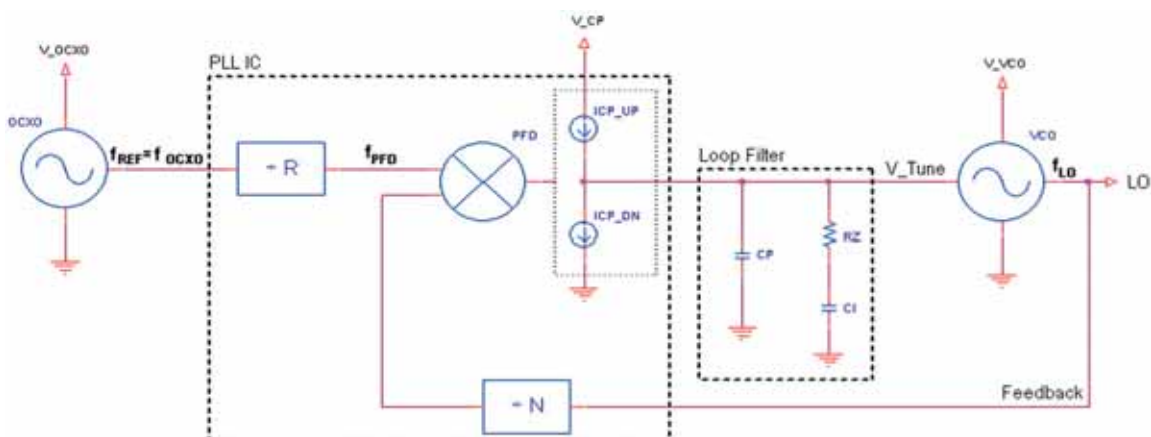


Figure 1: Basic building blocks of a PLL

cycle. However, doing this would create a “dead zone” in the loop response, as there is a significant drop in the small-signal loop gain – practically an open loop.

This dead zone is eliminated by forcing ICP_UP and ICP_DN to produce extremely narrow pulses during every PFD cycle. These are commonly referred to as anti-backlash pulses. This produces energy content on the VCO tune line at f_{PFD} and its harmonics. The negative feedback cannot counteract these pulses since these frequencies are outside the loop bandwidth of a properly designed PLL. The VCO then is frequency modulated (FM) by this energy content, and related spurs appear at f_{PFD} and its harmonics, all centered around LO.

Between anti-backlash pulses the charge pump current sources are off (tri-stated). Inherently, the charge pump has some leakage current when tri-stated. Using an op-amp in an active loop filter (such as in Figure 7) introduces yet another

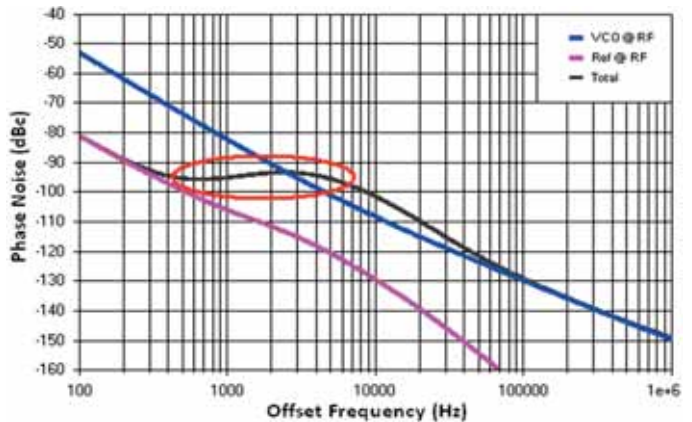


Figure 2: PLL IC phase noise contribution region as highlighted by the drawn ellipse

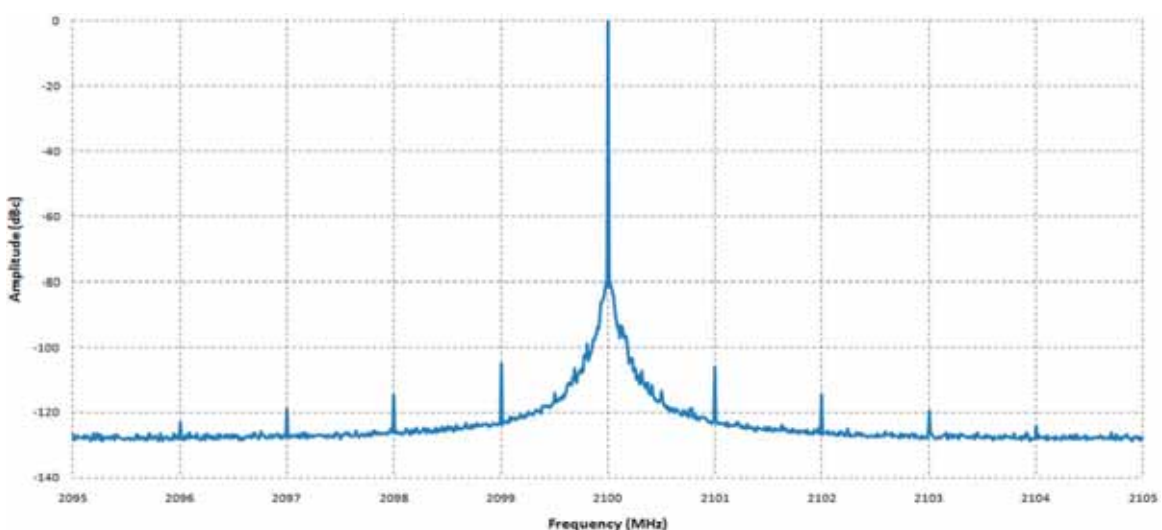


Figure 3: Reference spurs of a 2100MHz LO signal with an FPF of 1MHz generated using the LTC6945 PLL IC from Linear Technology along with the UMX-586-D16-G VCO from RFMD

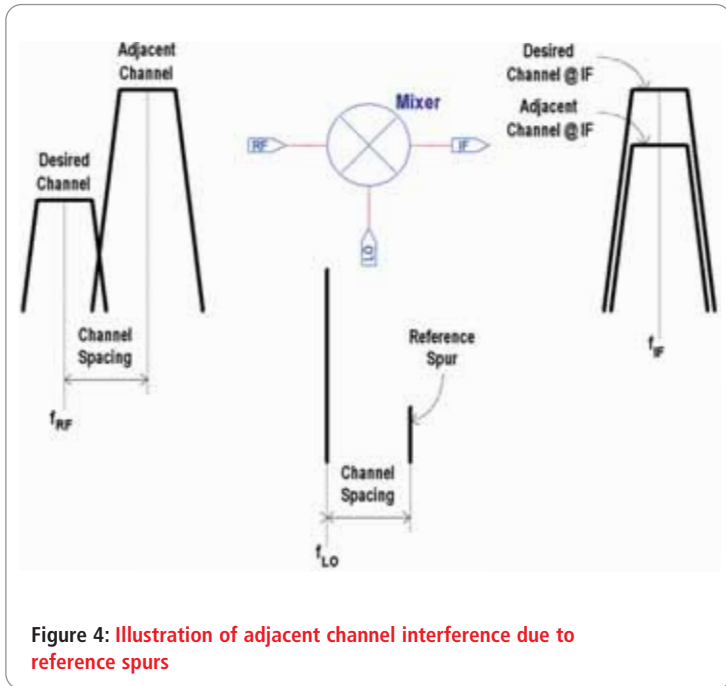


Figure 4: Illustration of adjacent channel interference due to reference spurs

leakage current source due to the op-amp's input bias and offset currents. The aggregate of these unwanted currents, whether sourcing or sinking, causes a drift in the voltage across the loop filter and, consequently, in the tune voltage of the VCO.

The negative feedback of the loop will correct for this anomaly by introducing a unipolar current pulse from the charge pump once every PFD cycle so that the average tune line voltage produces the correct frequency out of the VCO. The pulses produce energy at f_{PFD} , which also causes spurs to appear centered around LO and offset by f_{PFD} and its harmonics as previously noted.

In integer-N PLLs f_{PFD} is often chosen to be relatively small because of the system's frequency step size requirements. This means that the anti-backlash pulse width, especially with the present high-speed IC technologies, is extremely small compared to the PFD period. As such, a large leakage current causes the total charge pump pulses to be unipolar and tends to be the dominant cause of reference spurs. This phenomenon will be examined in more depth later on.

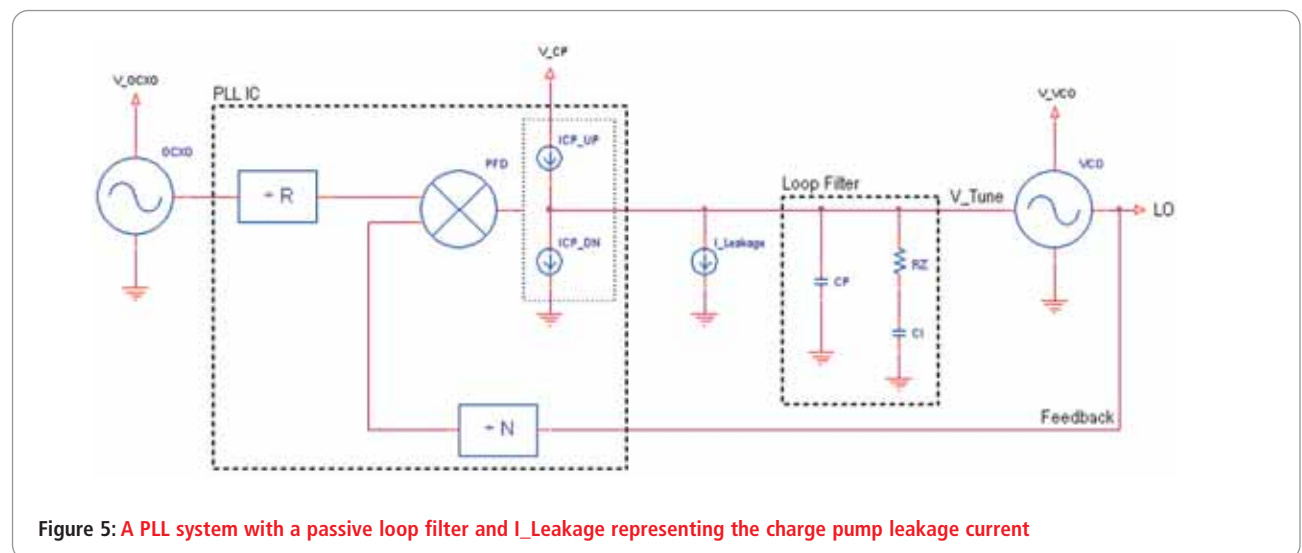


Figure 5: A PLL system with a passive loop filter and $I_{Leakage}$ representing the charge pump leakage current

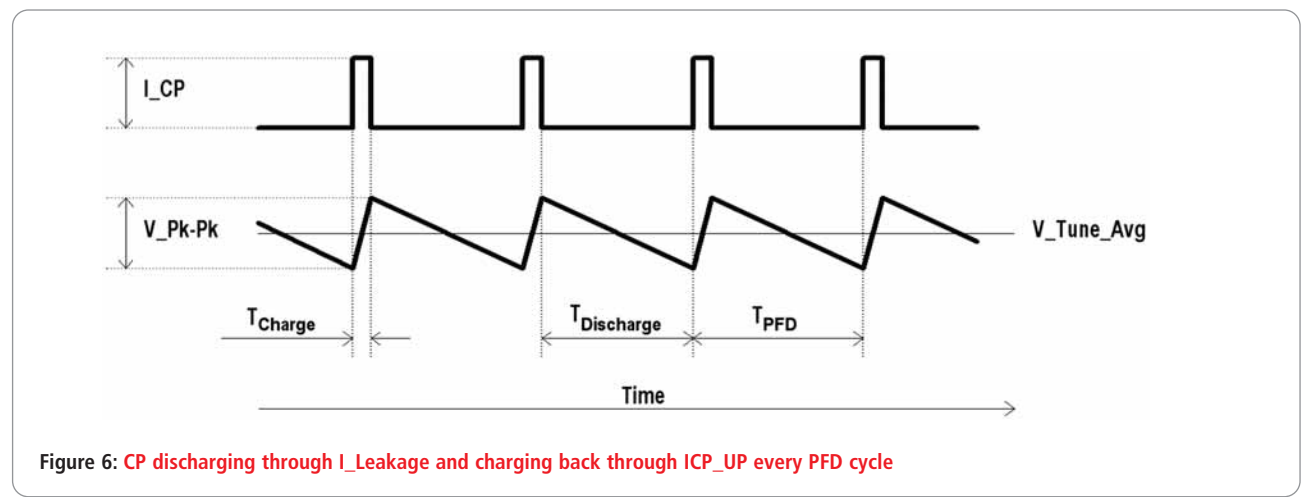


Figure 6: CP discharging through $I_{Leakage}$ and charging back through ICP_{UP} every PFD cycle

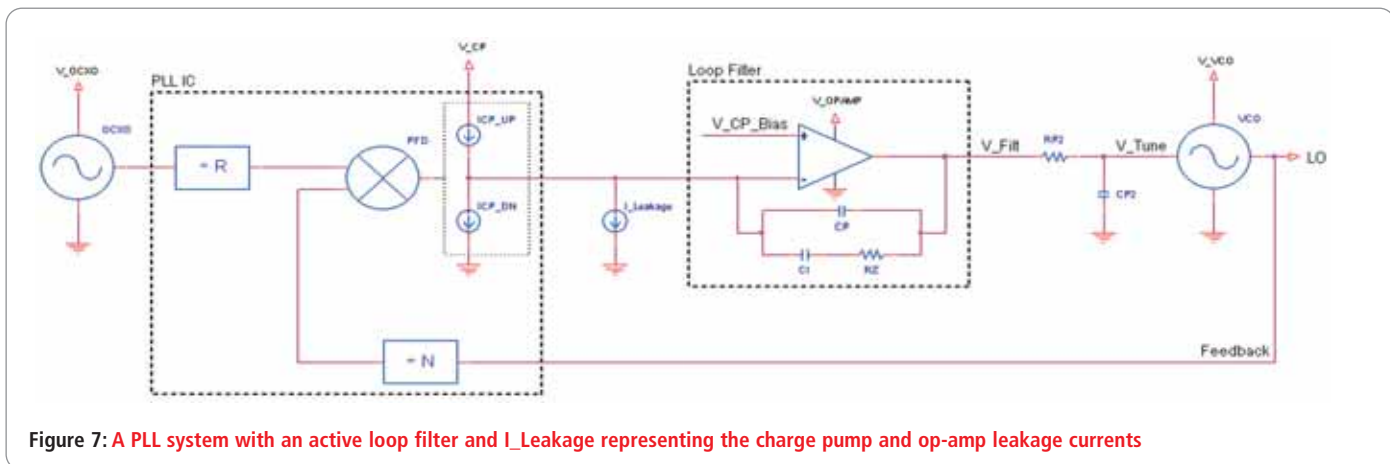


Figure 7: A PLL system with an active loop filter and I_{Leakage} representing the charge pump and op-amp leakage currents

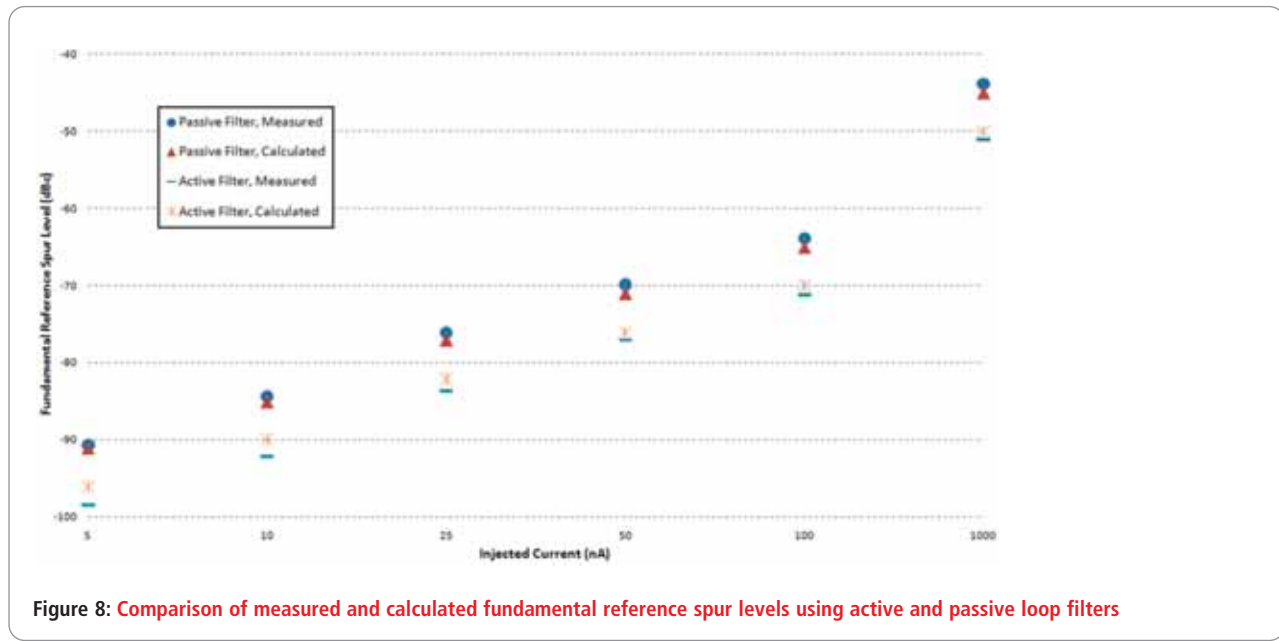


Figure 8: Comparison of measured and calculated fundamental reference spur levels using active and passive loop filters

Reference Spurs' Effect on System Performance

In a particular communications frequency band there are multiple channels that occupy equal bandwidths. The centre-to-centre frequency distance between two adjacent channels is equal among all channels and is denoted by channel spacing. Due to several factors, it is common to find large variations in signal strength between any two adjacent channels.

A typical scenario in a multi-channel wireless communications system, where a stronger channel exists adjacent to the desired but weaker channel, is shown in Figure 4. Only one of the LO reference spurs of concern is shown.

In an integer-N PLL f_{PFD} is usually chosen to be equal to the channel spacing, which means that the reference spurs are positioned at the channel spacing from the LO. These spurs translate all adjacent and nearby channels to the centre of the intermediate frequency (f_{IF}) along with the LO mixing the desired channel to the same frequency. These undesired

channels, being uncorrelated to the signal in the desired channel, appear as an elevated noise floor to the desired signal and limit the signal-to-noise ratio.

Relationship between Leakage Current and Reference Spur Levels

The mathematical prediction of a PLL IC's phase noise contribution is relatively straightforward and can be accurately determined by calculations. However, the prediction of reference spur levels is traditionally believed to be complex. This section derives a method to accurately predict reference spur levels due to leakage current using simple calculations. Two examples using different loop filters will be examined.

Passive Loop Filter Example

A PLL system with a typical passive loop filter is shown in Figure 5, along with a current source denoted I_{Leakage} to represent the leakage current of the charge pump. Assuming

the PLL is locked, I_{Leakage} reduces the charge held by C_p during the charge pump's off-time. When the charge pump turns on once every PFD cycle, $I_{\text{CP_UP}}$ replenishes the charge lost from C_p by applying a short pulse of current. Feedback forces the average voltage seen at V_{Tune} ($V_{\text{Tune_Avg}}$) to be constant, maintaining the correct LO frequency. Figure 6 depicts this.

The derivation of the resultant spurs involves some knowledge of loop stability requirements, the first being LBW restrictions. The LBW of the PLL system is designed to be at least 10 times smaller than f_{PFD} :

$$LBW \leq \frac{f_{\text{PFD}}}{10}.$$

This means that the period of the PFD is:

$$T_{\text{PFD}} = \frac{1}{f_{\text{PFD}}} \text{ and, hence, } LBW \leq \frac{1}{10 \cdot T_{\text{PFD}}}.$$

To create a stable loop with plenty of phase margin, a zero consisting of R_z and C_i in Figure 5 is inserted in the loop at about $1/3^{\text{rd}}$ the LBW. That is:

$$\text{Zero Location} \approx \frac{LBW}{3} = \frac{1}{2\pi\tau_z} \Rightarrow LBW \approx \frac{3}{2\pi\tau_z}, \text{ where } \tau_z = R_z \cdot C_i.$$

Replacing LBW in the last equation with its equivalent in terms of T_{PFD} results in:

$$\frac{3}{2\pi\tau_z} \leq \frac{1}{10 \cdot T_{\text{PFD}}}, \text{ or } T_{\text{PFD}} \leq \frac{2\pi}{30} \tau_z.$$

This means that the PFD period is almost five times shorter than the time constant of the zero, τ_z . This implies that the ripple produced at a period of T_{PFD} across C_p is mostly unseen by C_i . The closed-loop bandwidth LBW is approximately equal to the unity crossing of the open-loop gain. Since the zero is located within the loop bandwidth (it is located at $1/3^{\text{rd}}$ the unity crossing of the open-loop gain), the voltage across C_i is dictated by the negative feedback and is mostly a DC value. Practically speaking only C_p is discharged and charged during the PFD cycles shown in Figure 6.

If a capacitor C is charged or discharged with a constant current source I over a period of time given by ΔT , the voltage delta across this capacitor is given by:

$$\Delta V = I \frac{\Delta T}{C}.$$

To maintain a fixed output frequency at LO, the voltage droop that occurs during the discharge period is equal to the voltage buildup during the charging period of Figure 6. That is:

$$V_{\text{Pk-Pk}} = \frac{I_{\text{Leakage}} \cdot T_{\text{Discharge}}}{C_p} = \frac{I_{\text{CP}} \cdot T_{\text{Charge}}}{C_p},$$

where T_{Charge} is the amount of time the charge pump current is active during every PFD cycle.

The charge pump current I_{CP} is usually in the mA range and I_{Leakage} is usually in the nA range, which means that:

$$T_{\text{charge}} \ll T_{\text{PFD}} \text{ and } T_{\text{Discharge}} \approx T_{\text{PFD}}.$$

This implies that the ripple voltage seen across C_p can be represented by a sawtooth waveform.

To study the effect of this sawtooth waveform on the spectrum of the LO signal, and since the waveform is a periodic function, it can be broken down into its frequency components using Fourier Series analysis:

$$\text{Sawtooth Fourier Series} = \text{DC Value} - \frac{V_{\text{Pk-Pk}}}{\pi} \sum_{n=1}^{\infty} \frac{\sin(2\pi n f t)}{n},$$

where:

$$V_{\text{Pk-Pk}} = \frac{I_{\text{Leakage}} \cdot T_{\text{PFD}}}{C_p} = \frac{I_{\text{Leakage}}}{C_p \cdot f_{\text{PFD}}}.$$

When $n = 1$, the fundamental peak is:

$$V_{\text{pk-Fund}} = \frac{I_{\text{Leakage}}}{\pi C_p \cdot f_{\text{PFD}}},$$

the 2^{nd} harmonic peak is:

$$V_{\text{pk-2ndHar}} = \frac{I_{\text{Leakage}}}{2\pi C_p \cdot f_{\text{PFD}}}$$

and so on.

The DC value, which is equal to $V_{\text{Tune_Avg}}$ in Figure 6, is set by the negative feedback per the requested LO frequency. The AC components however frequency-modulate the VCO through its tune pin with a tuning sensitivity of K_{VCO} , to produce dual sideband spurs with a fundamental of f_{PFD} .

The box entitled 'Derivation of Spur-to-Carrier Ratio Using Narrowband FM Equations' derives the following equation that is going to be used next:

$$\frac{\text{Sideband}}{\text{Carrier}} = 20 \log_{10} \left(\frac{K_{\text{VCO}} \cdot E_m}{2f_m} \right).$$

The effect of the negative feedback on these AC components is negligible because f_{PFD} , being the fundamental and the lowest frequency component, is at least 10 times higher in frequency than the zero-dB crossing of the open-loop gain by design.

To find the fundamental reference spur-to-carrier power ratio, $f_m = f_{\text{PFD}}$, $E_m = V_{\text{pk-Fund}}$ and:

$$\frac{\text{Ref_Spur_Fund}}{\text{Carrier}} = 20 \log_{10} \left(\frac{K_{\text{VCO}} \cdot I_{\text{Leakage}}}{2\pi C_p \cdot f_{\text{PFD}}^2} \right), \text{ dBc.}$$

For the 2^{nd} harmonic reference spur, $f_m = 2 f_{\text{PFD}}$, $E_m = V_{\text{pk-2ndHar}}$ and:

$$\frac{\text{Ref_Spur_2ndHar}}{\text{Carrier}} = 20 \log_{10} \left(\frac{K_{\text{VCO}} \cdot I_{\text{Leakage}}}{8\pi C_p \cdot f_{\text{PFD}}^2} \right), \text{ dBc.}$$

Ratios for higher-order harmonics are found using a similar approach.

	Passive Loop Filter	Active Loop Filter
PLL IC	LTC6945, 6 GHz Integer-N Synthesizer from Linear Technology	LTC6945, 6 GHz Integer-N Synthesizer from Linear Technology
Op-Amp	N/A	LT1678, Low Noise, Rail-to-Rail Precision Op-Amp from Linear Technology
VCO	CVCO55CL-0902-0928, 902 to 928 MHz VCO from Crystek	UMS-1400-A16-G, 700-1400 MHz VCO from RFMD
C_P (nF)	8.2	22
f_{PFD} (kHz)	250	250
K_{VCO} (MHz/V)	18	63
LBW (kHz)	7	7.6
R_{P2} (Ohms)	N/A	100
C_{P2} (nF)	N/A	13.3

Table 1: PLL system details used to produce the comparison data of Figure 8 summary of results

Loop Filter Type	Passive	Active
Reference to	Figure 5	Figure 7
Ref_Spur_Fund Carrier (dBc)	$20 \log_{10} \left(\frac{K_{VCO} \cdot I_{Leakage} \cdot \left \frac{V_{Tune}}{V_{Filt}} \right _1}{2\pi C_p \cdot f_{PFD}^2} \right)$	
$\left \frac{V_{Tune}}{V_{Filt}} \right _1$	1	$\left \frac{1}{1 + j2\pi \cdot f_{PFD} \cdot R_{P2} \cdot C_{P2}} \right $
Ref_Spur_2ndHar Carrier (dBc)	$20 \log_{10} \left(\frac{K_{VCO} \cdot I_{Leakage} \cdot \left \frac{V_{Tune}}{V_{Filt}} \right _2}{8\pi C_p \cdot f_{PFD}^2} \right)$	
$\left \frac{V_{Tune}}{V_{Filt}} \right _2$	1	$\left \frac{1}{1 + j4\pi \cdot f_{PFD} \cdot R_{P2} \cdot C_{P2}} \right $
Ref_Spur_3rdHar Carrier (dBc)	$20 \log_{10} \left(\frac{K_{VCO} \cdot I_{Leakage} \cdot \left \frac{V_{Tune}}{V_{Filt}} \right _3}{18\pi C_p \cdot f_{PFD}^2} \right)$	
$\left \frac{V_{Tune}}{V_{Filt}} \right _3$	1	$\left \frac{1}{1 + j6\pi \cdot f_{PFD} \cdot R_{P2} \cdot C_{P2}} \right $

Table 2: Summary of equations to predict reference spur levels up to the 3rd harmonic

Active Loop Filter Example

Figure 7 shows an example implementation of an active loop filter built around an op-amp. $I_{Leakage}$ represents the combined leakage currents of the charge pump and the op-amp. The same methodology used in the passive filter example applies here since the loop filters have a similar structure.

The addition of the pole composed of R_{P2} and C_{P2} at the output of the op-amp to limit the device's contribution of noise beyond 15 or 20 times the LBW reduces the amplitude

of the sawtooth signal seen at the tuning node of the VCO. It should be noted that C_{P2} includes the input capacitance of the VCO tune port.

The sawtooth signal undergoes low-pass filtering whose equation can be found using basic voltage division equations in the Laplace Transform domain and can be written as:

$$\left| \frac{V_{Tune}}{V_{Filt}} \right| = \left| \frac{1}{1 + j2\pi f \cdot R_{P2} \cdot C_{P2}} \right|$$

Derivation of Spur-to-Carrier Ratio Using Narrowband FM Equations

Consider an FM signal centered at an LO of frequency f_c in Hz. This signal can be written as:

$$e(t) = E_c \cos(2\pi f_c t + \theta(t)),$$

where E_c is the peak amplitude of $e(t)$ in V.

The instantaneous frequency of $e(t)$ is:

$$\omega_{inst} = \frac{d}{dt}(2\pi f_c t + \theta(t)) = 2\pi f_c + \theta'(t), \text{rad/sec.}$$

Since $e(t)$ is an FM signal, the modulating signal $e_m(t)$ modulates the instantaneous frequency of $e(t)$ as follows:

$$\theta'(t) = K e_m(t), \text{rad/sec.}$$

where K is the deviation sensitivity of frequency in rad/(sec·V).

$$\theta(t) = \int_0^t \theta'(t) dt = \int_0^t K e_m(t) dt = K \int_0^t e_m(t) dt.$$

As far as this paper is concerned, the modulating signal is a tone – one of the Fourier Series components of the sawtooth waveform – which is given by:

$$e_m(t) = E_m \cos(2\pi f_m t),$$

where E_m is the peak amplitude of $e_m(t)$ in V and f_m is its frequency in Hz.

This means that the time-varying component of $e(t)$'s phase is:

$$\theta(t) = K \int_0^t E_m \cos(2\pi f_m t) dt = \frac{K \cdot E_m}{2\pi f_m} \sin(2\pi f_m t) = \frac{2\pi K_{VCO} \cdot E_m}{2\pi f_m} \sin(2\pi f_m t),$$

where K_{VCO} , in Hz/V, is the tuning sensitivity of the VCO used to generate $e(t)$. Define m as the modulation index, such as:

$$\theta(t) = \frac{K_{VCO} \cdot E_m}{f_m} \sin(2\pi f_m t) = m \cdot \sin(2\pi f_m t), \text{where } m = \frac{K_{VCO} \cdot E_m}{f_m}.$$

$e(t)$, then, can be written as:

$$e(t) = E_c \cos(2\pi f_c t + m \cdot \sin(2\pi f_m t)).$$

Expanding using some basic trigonometric identities gives:

$$e(t) = E_c \cos(2\pi f_c t) \cdot \cos(m \cdot \sin(2\pi f_m t)) - E_c \sin(2\pi f_c t) \cdot \sin(m \cdot \sin(2\pi f_m t)).$$

where m is much smaller than 1 as far as the reference spur generation is concerned. This implies that:

$$\cos(m \cdot \sin(2\pi f_m t)) \approx 1$$

and $\sin(m \cdot \sin(2\pi f_m t)) \approx m \cdot \sin(2\pi f_m t)$.

Then:

$$e(t) \approx E_c \cos(2\pi f_c t) - m \cdot E_c \sin(2\pi f_c t) \cdot \sin(2\pi f_m t),$$

or:

$$e(t) = E_c \cos(2\pi f_c t) + \frac{1}{2} m \cdot E_c (\cos(2\pi(f_c + f_m)t) - \cos(2\pi(f_c - f_m)t)),$$

which is a narrow-band FM signal composed of a carrier at f_c and two sidebands located at $\pm f_m$ centered around the carrier.

Based on the last representation of $e(t)$, sideband-to-carrier power ratio in dBc is given by:

$$\frac{\text{Sideband}}{\text{Carrier}} = 20 \log_{10} \left(\frac{m}{2} \right) = 20 \log_{10} \left(\frac{K_{VCO} \cdot E_m}{2f_m} \right).$$

where f represents frequency in Hz.

Naturally, the sawtooth signal's Fourier Series components get affected differently according to their frequency. The reference spur-to-carrier ratios become:

$$\frac{\text{Ref_Spur_Fund}}{\text{Carrier}} = 20 \log_{10} \left(\frac{K_{VCO} \cdot I_{\text{Leakage}} \cdot \left| \frac{V_{\text{Tune}}}{V_{\text{Filt}}} \right|_1}{2\pi C_p \cdot f_{\text{PFD}}^2} \right), \text{dBc, where}$$

$$\left| \frac{V_{\text{Tune}}}{V_{\text{Filt}}} \right|_1 = \left| \frac{1}{1 + j2\pi \cdot f_{\text{PFD}} \cdot R_{P2} \cdot C_{P2}} \right|$$

$$\frac{\text{Ref_Spur_2ndHar}}{\text{Carrier}} = 20 \log_{10} \left(\frac{K_{VCO} \cdot I_{\text{Leakage}} \cdot \left| \frac{V_{\text{Tune}}}{V_{\text{Filt}}} \right|_2}{8\pi C_p \cdot f_{\text{PFD}}^2} \right), \text{dBc, where}$$

$$\left| \frac{V_{\text{Tune}}}{V_{\text{Filt}}} \right|_2 = \left| \frac{1}{1 + j4\pi \cdot f_{\text{PFD}} \cdot R_{P2} \cdot C_{P2}} \right|, \text{and so on.}$$

Lab Verification of the Theory

The PLL systems shown in Figures 5 and 7 were reproduced in the lab. External current was introduced at the charge pump node using a precision source meter to null the intrinsic fundamental reference spur caused by inherent leakages in the system. Then, specific additional current values were injected into the loop while measuring the fundamental reference spur levels.

Figure 8 compares the measured and calculated values for both filter types. The measured and calculated numbers agree to within the instrument accuracies and component tolerances. Table 1 presents more details about the PLL systems used to generate the measurements of Figure 8.

Important Topics

Integer-N PLL operation and non-idealities are important topics in the design of RF systems. Reference spurs can have a significantly negative impact on overall system performance. A simple yet accurate model to predict reference spur levels due to leakage current in PLLs can be a useful tool, saving time and board revisions. Measurements taken using example circuits verified the accuracy of this derived model. ●

References:

1. B. P. Lathi, "Modern Digital and Analog Communication Systems", Third Edition, Oxford University Press, 1998, ISBN 0195110099
2. F. M. Gardner, "Phaselock Techniques", Third Edition, John Wiley and Sons, 2005, ISBN 0471430633
3. Linear Technology, LTC6945 Datasheet, 1630 McCarthy Blvd., Milpitas, CA, 95035, www.linear.com
4. R. E. Best, "Phase-Locked Loops, Theory, Design, and Applications", Second Edition, McGraw-Hill, 1993, ISBN 0079113869
5. W. F. Egan, "Frequency Synthesis by Phase Lock", Second Edition, John Wiley and Sons, 2000, ISBN 0471321044
6. Z. Tranter, "Principles of Communications, Systems, Modulation, and Noise", Fourth Edition, John Wiley and Sons, 1995, ISBN 0471124966

1U MULTI-RANGE PROGRAMMABLE DC POWER SUPPLIES PWX Series



TELONIC
www.telonic.co.uk info@telonic.co.uk
 Tel : 01189 786 911 Fax : 01189 792 338

KIKUSUI
www.kikusui.com
 Tel : 01189 786 911 Fax : 01189 792 338

POWER-SAVING SCHEME FOR VIDEO-ON-DEMAND SERVICES IN IPTV

IKRAM SYED AND HOON KIM OF THE UNIVERSITY OF INCHEON IN KOREA DESCRIBE AN EFFICIENT POWER-SAVING SCHEME FOR VOD SERVICES, TAKING INTO ACCOUNT THE DOWNLOAD AND PLAYBACK TIME OF THE CONTENT

Recently, there has been a rapid growth in the demand for Internet Protocol television (IPTV) services, and video on demand (VOD) is one of its most prominent. A Cisco forecast indicates that total video traffic, including TV and VOD, will account for over 91% of global consumer traffic by 2014. The report also states that VOD traffic would have doubled every two and a half years through to 2014. However, the IP network is also one of the highest contributors to energy consumption and, as such the development of an energy-efficient system is seen as a very important research area.

VOD Power Consumption

VOD is a service which allows users to browse, select and watch videos and other content over a network that is an IPTV. The content is generally retrieved from a server and delivered to the user. VOD services can be either streaming services, allowing viewing in real time, or downloading services, which are also known as download-and-play (DP). The DP delivery method is a form of progressive downloading within the client server architecture. With this method a portion of the video is downloaded from the VOD servers prior to playback, in order to ensure smooth and reliable streaming.

All of this requires a lot of power and most of the power is consumed in the transmission of VOD content.

There have been several proposals presented in the past regarding the improvement of power consumption in VOD systems. To date, system designers have analyzed the energy consumption arising from storing and transmission of VOD content. Their proposed schemes improved the energy efficiency significantly by placing the VOD systems in very energy-efficient positions within the network. Researchers C. A. Chan, E. Wong, A. Nirmalathas and J. Chamil presented energy-consumption models for VOD services delivered through localized hybrid peer-to-peer (HP2P) and localized peer-assisted patching (PAP) with multicast video delivery methods over optical access networks.

However, all these efforts did not consider the download or playback of the VOD content, as the download is completed at an early stage of the total VOD period. The motivation behind our work is to develop an efficient power-saving scheme for VOD services, which switches the power-consumption mode to power-saving mode immediately after the download of the VOD content is complete.

System Model

Figure 1 shows the basic IPTV architecture of a VOD service, which consists of a VOD server, storage server, IP network and a set-top box (STB). The STB converts the transmitted source signals into a signal that can be displayed on a television screen or other display device. The STB can be considered a collection of functional blocks or modules, as shown in Figure 2, where each module performs a defined task.

The front end of the STB consists of a tuner and a demodulator, as shown in the dashed box in Figure 2. The STB is tuned to select one of a number of frequencies. The demodulator converts the RF signal into the original signal.

In the conventional VOD delivery scheme, most of the STB modules remain turned on throughout the VOD period. However, when the download of the VOD content is complete and all VOD data has been transferred to the user's STB, there is no need to leave the receiver

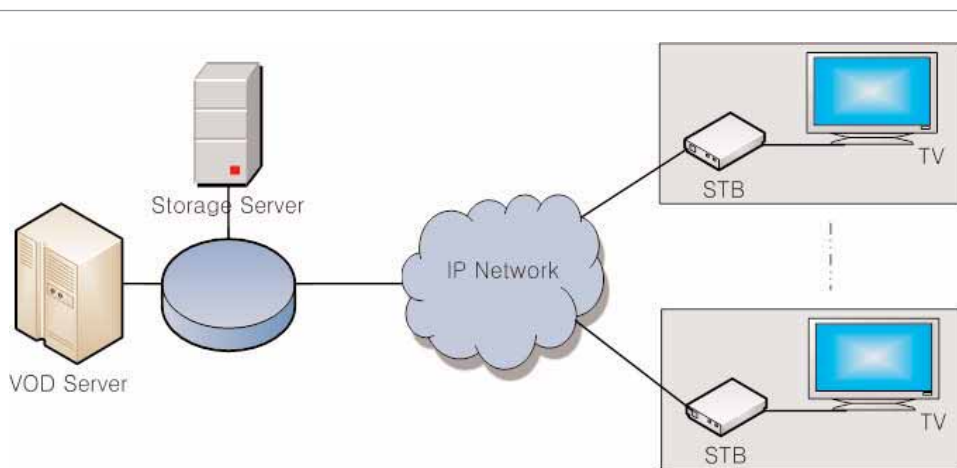
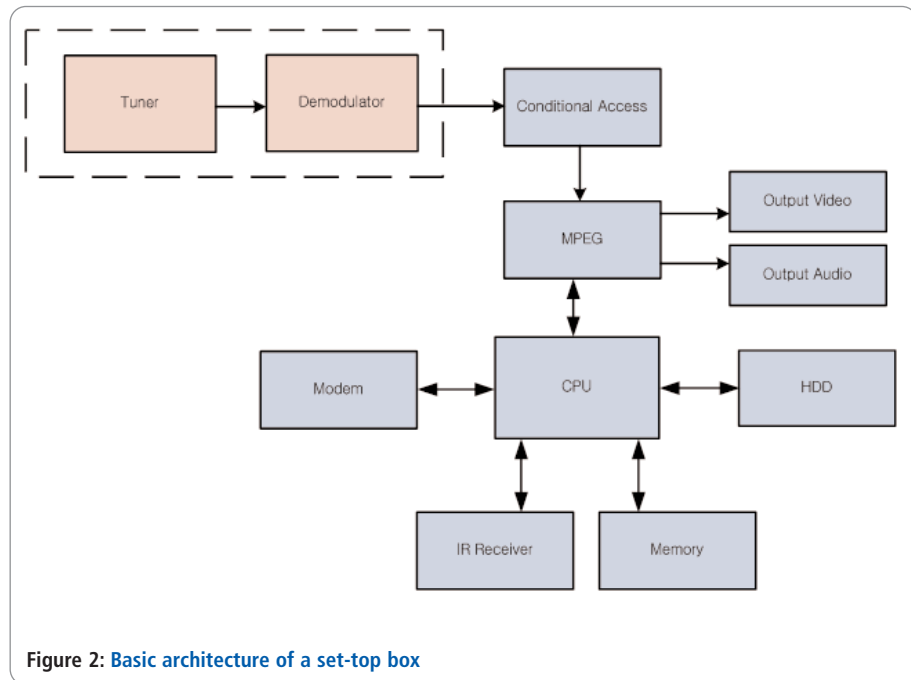


Figure 1: An IPTV architecture of a VOD service



modules (tuner and demodulator) turned on during playback. The download is usually completed much earlier than the end of the playback period and, therefore, the proposed scheme turns the receiver modules off after the VOD content has been transferred to the STB, improving the overall power efficiency of the VOD network.

Power Consumed by VOD Services

Here we will focus on two power schemes for VOD services: the conventional power consumption scheme and the proposed power-saving scheme.

The conventional scheme has two power-consumption modes, namely, an on mode and a stand-by mode. In the on mode, power is supplied to all STB modules and they perform their main functions. In stand-by mode power is supplied to all STB modules but here they do not perform their main functions and can be switched to a different mode by a remote controller or an internal signal.

The scheme we are suggesting has three power consumption modes: on mode, power-saving mode and a stand-by mode. In the power-saving mode, power is supplied to all STB modules, except the receiver (tuner and demodulator), and so the STB modules perform their main functions. During the download of VOD content, all the STB modules are in the on mode, consuming power. As the VOD content is transferred to the STB, the proposed scheme switches from power-consumption mode to a power-saving mode, by turning off the receiver modules (tuner and demodulator). As a result, the proposed scheme saves power that would usually be consumed by the receiver modules during playback. Figure 3 shows the flow chart of the proposed scheme.

Figure 4 shows the power consumption for different modes of the conventional and proposed schemes at times T_0 , T_1 , T_2 , T_3 and T_4 . T_0 denotes the time at which the download of VOD content begins; it is found that both the conventional and the proposed schemes consume on-mode power from the time period T_0 to T_2 . At time T_2 , the download of the VOD content is complete and the entire VOD content is transferred to the user's STB.

The conventional scheme remains in the on-mode for the

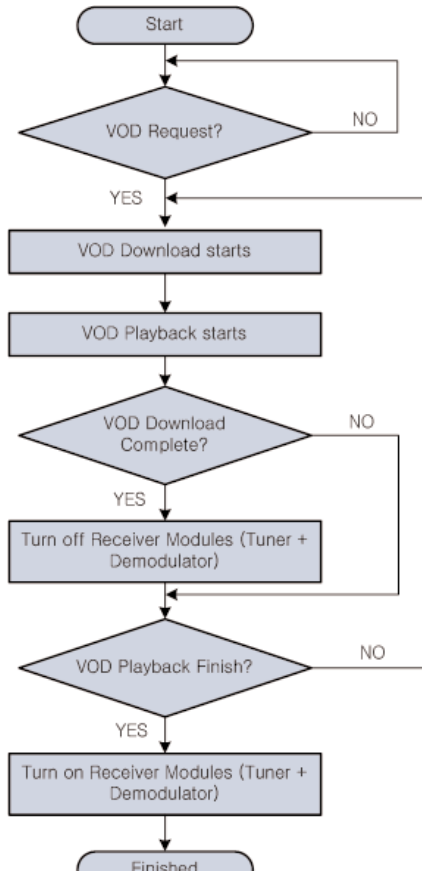
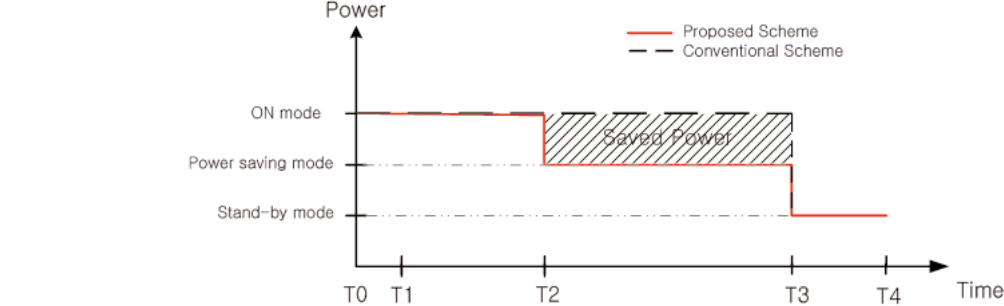
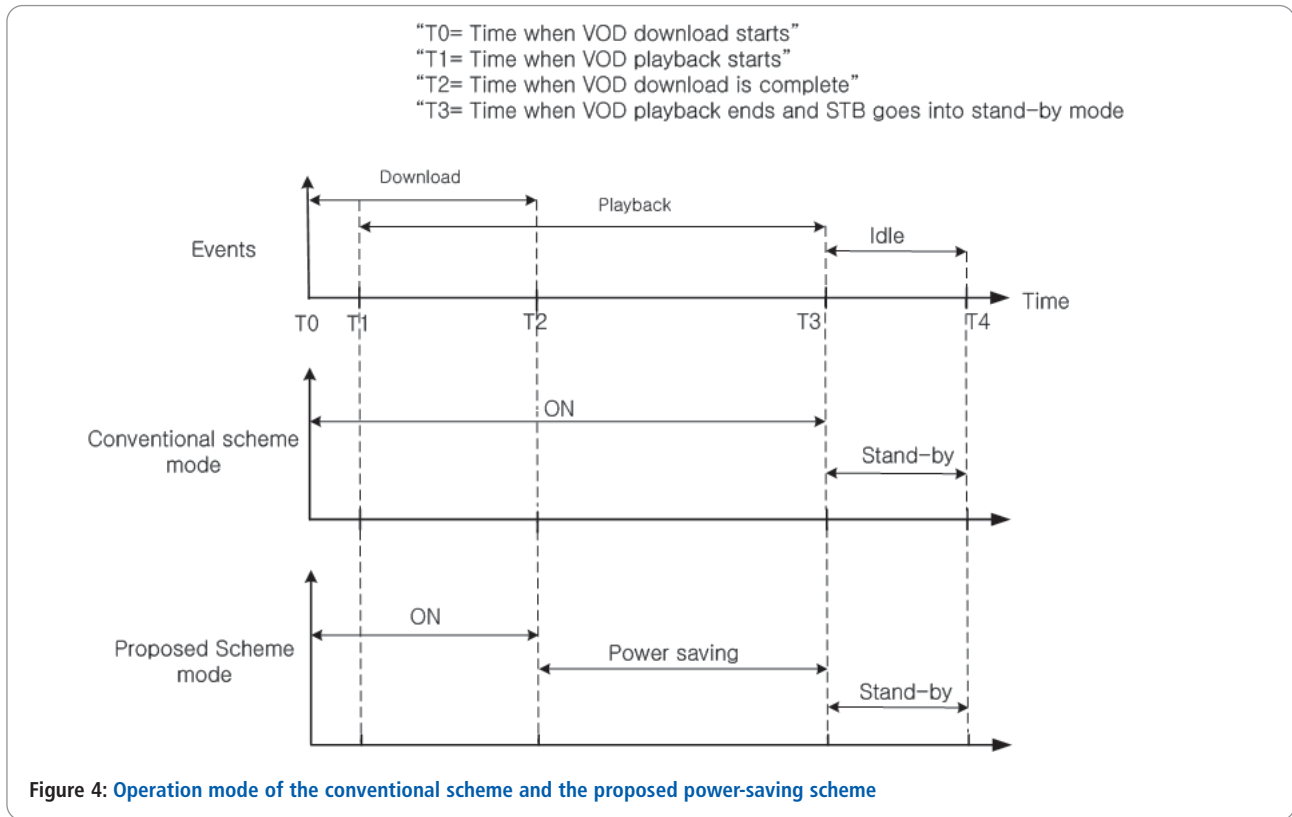


Figure 3: Flow chart for the proposed scheme transition from on mode to the power-saving mode



total VOD period and consumes on-mode power for the full duration, even though there is no need for the receiver modules to remain active during playback. Our scheme switches from power-consumption mode to power-saving mode by turning off the receiver modules (tuner and demodulator) immediately after the download is complete. The proposed scheme therefore saves power that would usually be consumed by the receiver modules during the playback period, improving the overall power consumption of the VOD service.

Figure 5 shows a comparison of the power consumption for both schemes for the total VOD period. The dotted line shows the power consumed by the conventional scheme, whereas the red line shows the power consumed by the proposed power-saving scheme.

Performance Evaluation

Performance evaluation depends on the network used by

the subscriber. For the performance evaluation we use the available broadband networks (XDSL, cable, FTTB and FTTH), each having different upload and download rates, as shown in Table 1.

Researchers Y. J. Won, M. Choi, B. C. Park and J. W. Hong summarize the VOD and download times, along with the VOD size associated with one episode of a popular TV series 'CSI

Network Type	Download Rate	Upload Rate
XDSL	6.8 Mbps	415 Kbps
Cable	59.7 Mbps	2.5 Mbps
FTTB	91.9 Mbps	93.5 Mbps
FTTH	78.8 Mbps	94 Mbps

Table 1: Available broadband network data rates

Networks Type	VOD Size	VOD Time (TVOD)	Download Time (TDL)
XDSL	792Mbytes	46min	20min
Cable	1931Mbytes	89min	43min
FTTB	810Mbytes	42min	14min
FTTH	833Mbytes	42min	13min

Table 2: VOD time and download time for the given VOD

Mode	Average Power (W)	Max Power (W)	Min Power (W)
P_{ON}	13.2	20.9	6.6
SB (stand-by)	9.5	19.4	2.2
PPS (proposed power saving)	10.2	17.9	3.6

Table 3: STB power consumption in different operational modes

Miami' in Table 2. From this table, it is found that the download time TDL depends on the VOD content size and the network type, whereas the total VOD time TVOD depends on the quality of the VOD content. Further, it is clear that the download of the VOD content is completed at an early stage of the total VOD period. For an average of 40 minutes of playback time, the download time is around 13-20min, which is less than 50% of the total VOD time.

The performance of both the schemes is evaluated on the basis of the power consumed during the total VOD period by using the power equations. TEC denotes the total energy consumption, defined by the average power consumption in a year, and TEC_j denotes the TEC in kilowatt-hours per year for the conventional scheme. TEC_j is computed as follows:

$$TEC_j = (T_{ON}^j \cdot P_{ON} + T_{SB}^j \cdot P_{SB}) \times 0.365$$

P_{ON} and P_{SB} are the power consumption of the STB in watt-hours for the on-mode and the stand-by mode respectively, as shown in Table 3. T_{ON}^j is the on-mode time for the conventional scheme, which is equal to the total VOD time T_{VOD} , whereas T_{SB}^j is the stand-by mode time.

TEC_j is the energy consumed by the proposed power-saving scheme in kilowatt-hours per year and it can be computed as follows:

$$TEC_j = (T_{ON}^j \cdot P_{ON} + T_{PS}^j \cdot P_{PS} + T_{SB}^j \cdot P_{SB}) \times 0.365$$

P_{ON} is considered to be the maximum power consumed by the STB during the VOD period and P_{PS} is the power consumed in the power-saving mode, when the download of the VOD content is completed. The power consumed in this

mode is calculated on the basis of the on-mode power, tuner power and demodulator power. The tuner consumes 2W, whereas the demodulator consumes 1W. T_{ON}^j is the on-mode time of the STB, whereas T_{PS}^j is the power-saving mode time of the proposed scheme.

$$T_{ON}^j = T_{DL}$$

while

$$T_{PS}^j = T_{VOD} - T_{DL}$$

The total power saving in a year can be calculated as:

$$TEC_S = ((T_{ON}^j - T_{ON}^j) \times P_{ON} - T_{PS}^j \cdot P_{PS}) \times 0.365$$

In Table 4, we evaluate the power consumed by the proposed scheme and compare it with the power consumed by the conventional scheme, on the basis of the above parameters. The evaluation results show that the proposed scheme provides significant power savings for VOD services compared to the conventional scheme. Given that the proposed scheme turns the receiver modules off immediately after the download of VOD content is complete, while the conventional scheme remains in the on mode for the total VOD period, the proposed scheme saves up to 15% of the total power consumed by the VOD services. ●

This work was supported by the Energy Efficiency & Resources at the Korea Institute of Energy Technology Evaluation and Planning (20102010100071, 'Development of low power set-top box').

Network Type	Power Consumption		Power Saving
	Conventional Scheme	Proposed Scheme	
XDSL	10.12W	8.82W	12.85%
Cable	19.58W	17.28W	11.75%
FTTB	9.24W	7.84W	15.15%
FTTH	9.24W	7.79W	15.69%

Table 4: Comparison of power consumed in both schemes



YONG TANG AND BIN YANG FROM THE COLLEGE OF AUTOMOBILE AND HONGBIN GU FROM THE COLLEGE OF CIVIL AVIATION AT CHINA, PRESENT A PROCESS THAT CREATES AND INCORPORATES DISPLAY EXPERIENCE

Creating a Realistic Virtual Hand For Head-Mounted Displays

Virtual reality (VR) applications are increasingly finding their way into head-mounted display (HMD) environments. Hands are the most effective interactive tool because of their manipulation flexibility, and HMD users prefer to maintain a constant visual contact with their hands. However, ensuring a real-time visualization of a virtual hand is not so easy.

Controlling a virtual hand requires the user to wear a motion sensor that detects hand movements, such as a data glove – currently the most popular and effective device for capturing hand gestures. Unfortunately, the data glove has drawbacks, including high cost and the sense of it not being realistic. As such, a number of studies are now focusing on vision-based hand-position estimation. However, although the data glove method provides a more natural, non-contact solution, so far it has only been used in the lab.

The visualization of a virtual hand requires building a 3D model of the user's hand, with the quality of the final image depending on the accuracy of that model. Equally, although an option, a generic 3D hand-model results in users describing it as not realistic enough too.

In order to see a more realistic hand, here we describe a method of visualizing user's hands through a simple, low-cost approach, based on augmented virtuality (AV) as shown in Figure 1. Two-dimensional camera images are integrated into the virtual environment in real time, which allow users to see realistic views of their hands in the HMD.

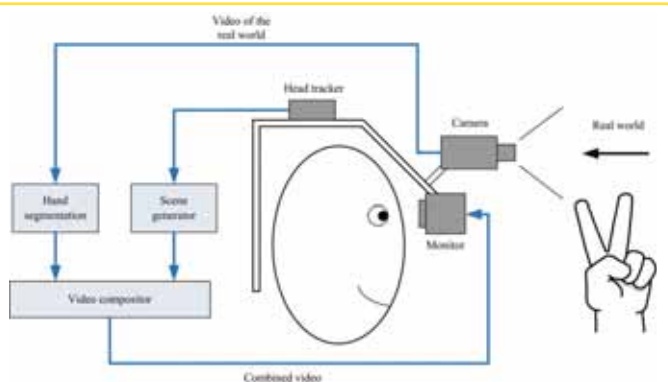


Figure 1: Architecture of the visualization of a virtual hand, based on augmented virtuality (AV)

Real-Time Hand Segmentation

'Extracting' the hand from the background, also known as segmentation, is an essential task for vision-based Hand-Computer Interaction (HCI) systems. A high recognition rate depends on the quality of the results from this process.

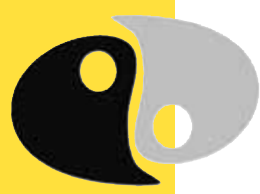
A so-called colour-based hand detection method has recently become popular because of its efficiency and precision. This method extracts the target object using colour information, so non-uniform objects, such as hands, faces and bodies can be easily acquired. As such, the colour-based detection method is found suitable for use in VR systems.

Capturing a frame in video, every pixel could fit in one of two categories: skin-coloured pixel or a non-skin-coloured pixel. Skin-coloured pixels are transformed from an RGB (red, green, blue) format into HSV (hue, saturation, value). HSV is another colour format like RGB, but the range of the 'value' is from 0 to 1. HSV is most common cylindrical-coordinate representations of points in the RGB colour model.

Following the transformation to HSV, the hue and saturation are used to create a Gaussian model to represent the skin-colour probability. Parameters of the model are generated from the sample, which uses the standard maximum-likelihood methods.

Positioning the cameras so they offer the same view as the eyes is, for now, impossible due to the physical constraints of the HMD systems. The virtual viewpoint was set in a virtual environment consisting of the positions of the cameras to ensure their registering in the VR system. As such, the distance between the cameras' positions and that of the eyes may result in inaccuracies and uncertainty of the user's impression. In order to eliminate the viewing distance, a view interpolation algorithm based on view morphing was used to generate virtual view images of the hand for each video frame, as shown in Figure 2.

Assuming I_0 is the image of the object and I_1 is its second image, the same two images can be produced by moving the camera instead of the object. A new perspective view could be produced by linear image interpolation when the camera moves in parallel to the image plane. Assuming the camera's position is moved from the original position's



AND TRAFFIC ENGINEERING AT NANJING FORESTRY UNIVERSITY NANJING UNIVERSITY OF AERONAUTICS AND ASTRONAUTICS, IMAGES OF USERS' HANDS TO IMPROVE THE HEAD-MOUNTED

THIS REGULAR FEATURE COVERS ISSUES RELATED TO CHINESE RESEARCH AND DEVELOPMENT (R&D)

coordinates $(C_x, C_y, 0)$, the focal length is changed from f_o to f_i .

The respective projection matrices of the cameras Π_o and Π_i can be written as follows:

$$\Pi_o = \begin{bmatrix} f_o & 0 & 0 & 0 \\ 0 & f_o & 0 & 0 \\ 0 & 0 & 1 & 0 \end{bmatrix}; \quad \Pi_i = \begin{bmatrix} f_i & 0 & 0 & -f_i C_x \\ 0 & f_i & 0 & -f_i C_y \\ 0 & 0 & 1 & 0 \end{bmatrix} \quad (1)$$

Assuming $p_o \in I_o$ and $p_i \in I_i$ are the projections of point $P = [X \ Y \ Z \ 1]^T$, then their linear interpolation yields the following:

$$(1-s)p_o + sp_i = (1-s)\frac{1}{Z}\Pi_o P + s\frac{1}{Z}\Pi_i P = \frac{1}{Z}\Pi_s P \quad (2)$$

where:

$$\Pi_s = (1-s)\Pi_o + s\Pi_i \quad (3)$$

Therefore, image interpolation produces an image of the new viewpoint with projection matrix Π_s , which is a linear interpolation of Π_o and Π_i . The centre C_s and the focal length f_s of the virtual camera are then given by:

$$C_s = (sC_x, sC_y, 0) \quad (4)$$

$$f_s = (1-s)f_o + sf_i \quad (5)$$

Consequently, the interpolated images from parallel cameras produce an illusion of continuously moving the camera in line $\overline{C_oC_i}$. Moreover, the algorithm is shape-

preserving because the image interpolation generates a new image of the same object. Setting the value for the interpolation parameter s_{hp} , the image is generated by line interpolation as shown in Figure 3.

Seamless Fusion of Real and Virtual Scenes

In an augmented reality (AR) system, maintaining the same camera parameters of the physical and virtual cameras is necessary to display the composed image correctly. Maintaining the correct registering of the real and virtual worlds includes intrinsic and extrinsic parameters.

A physical camera is stable, so a suitable virtual camera with the same intrinsic parameters was set. Taking several pictures of a chessboard (shown in Figure 4), with each image having different orientation, we can generate intrinsic parameters of this camera with Matlab's calibration tool.

Assuming the image's parameters as *height* and *width*, the intrinsic matrix K is given by focal lengths f_x , f_y and principal points u_0, v_0 . In computer graphics the projection model is defined as a viewing frustum P, which includes a horizontal viewing angle α , a vertical viewing angle β , a back clipping plane *far* and a front clipping plane *near*. From the geometric relationship shown in Figure 5, we can calculate α and β as:

$$\begin{aligned} \alpha &= \arctan(u_0/f_x) + \arctan((width - u_0)/f_x) \\ \beta &= \arctan(v_0/f_y) + \arctan((v_0 - height)/f_y) \end{aligned} \quad (6)$$

Extrinsic parameters also include the position of the camera. The physical camera is updated using head motions,

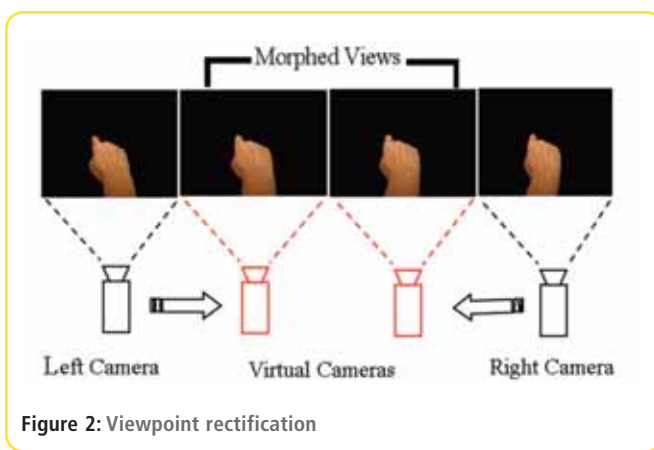


Figure 2: Viewpoint rectification

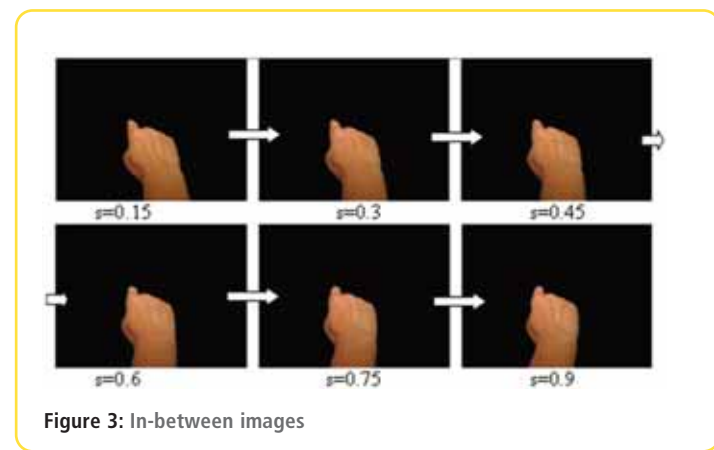


Figure 3: In-between images

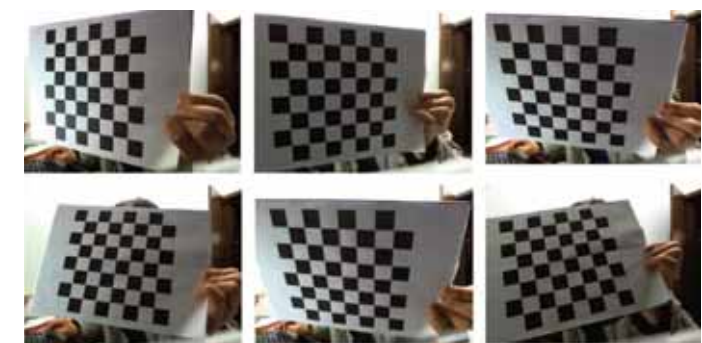


Figure 4: Various positions of the chessboard

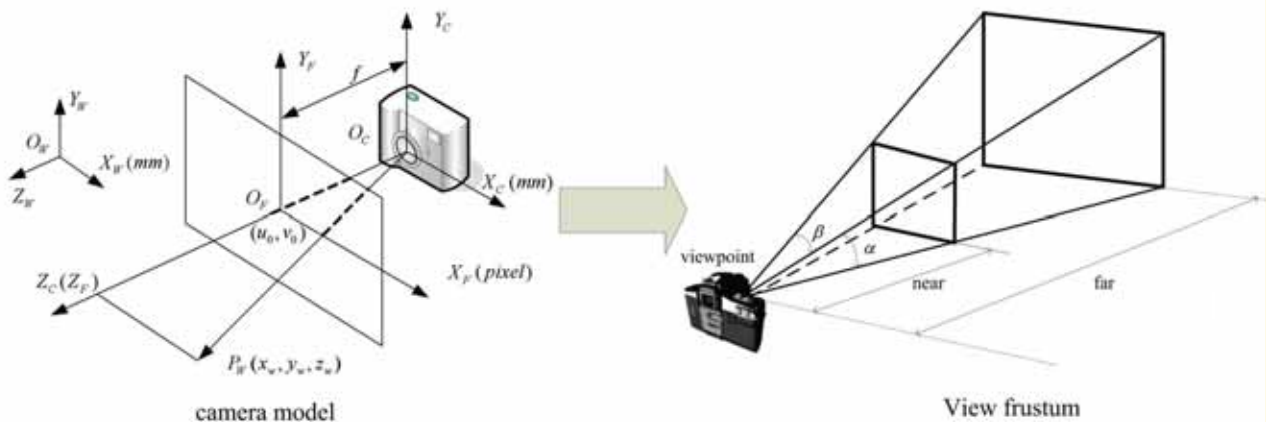


Figure 5: Conversion of the intrinsic parameters

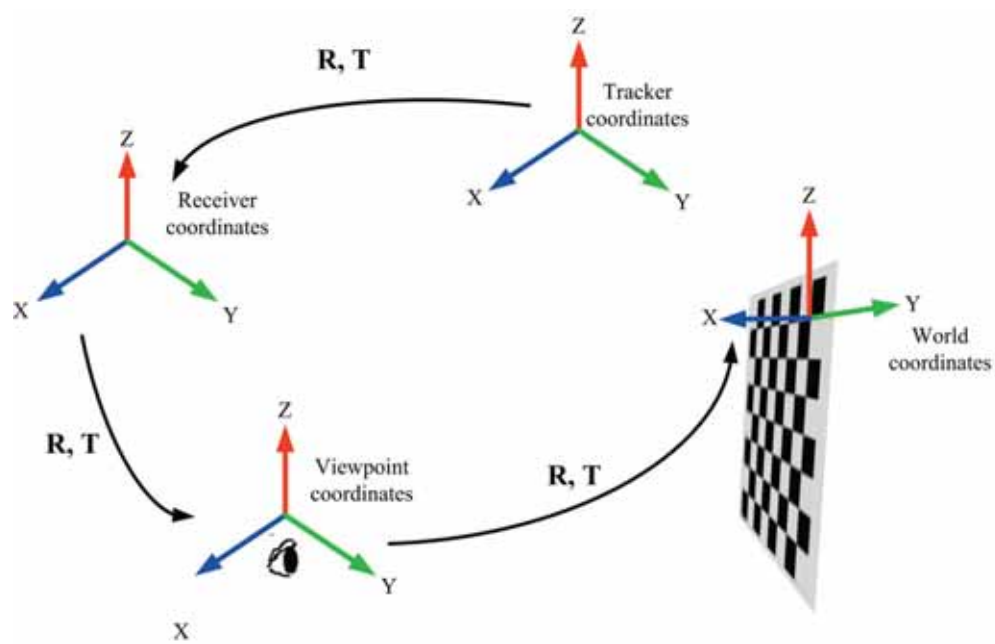
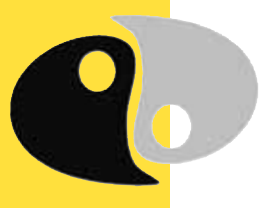


Figure 6: Coordinates' transformation



so the hand image, as an insert in the view, appears as spatially stable. In VR, we are then tracking the motion of the physical camera and driving the motion of the virtual camera. Coordinates' transformation should be used to convert the tracker data into defined coordinates, as the head tracker is fixed onto the HMD, which is at a distance from the physical camera. A corner on the chessboard was chosen as the origin of real-world coordinates, with the axis set along the first rectangle on the chessboard, as shown in Figure 6. Finding the translation vector T and rotation matrix R from the coordinates, we can realize the coordinates' conversion.

Alpha blending is used to integrate the segmented hand in the rendered view of the VR application and to show the user's hand in a virtual environment. The pixel value after blending c_d can be defined as:

$$c_d = \alpha \cdot c_a + (1 - \alpha)c_s \quad (7)$$

where α is from 0 to 1. For antialiasing, the pixels were classified as follows: If the pixel is in the contour, α is equal to 1; if the pixel is at boundary of the contour, α is equal to 0.5; for anything else, α is equal to 0.

The Experiment

A customized virtual reality system using VR1280 head mount display was used for the experiment. VR1280 is a display device with 1280×1024 resolution for advanced virtual reality applications. A USB camera with a resolution of 640×480 pixels and 60fps were attached onto the HMD. A PDI tracker was fixed on top of it.

The 3D scene was rendered using OpenGL (Open Graphics Library), which is a cross-language, multi-platform API for rendering 2D and 3D computer graphics. In the experiment, a 3D virtual cockpit environment was created within an inert model-based-rendering virtual hand and image-based-rendering virtual hand. The first virtual hand was a traditional 3D model, formed with many triangles, whereas the other virtual hand was the segmented image.

As shown in Figures 7 and 8, the visual presentation of the current method (b) appears more realistic than that of the traditional method (a). Moreover, data gloves or other equipment are not needed to drive the hand motion. Thus, the user feels it as more natural.

A hand interaction test was conducted to evaluate the ability of the user to complete the hand interaction task in VE. As shown in Figure 9, a chessboard sheet was placed on a wall and a similar one was created in the virtual environment. Participants had to touch the individual squares on the virtual sheet to evaluate whether the user

touched the correct square on the physical sheet or not. Experimental results showed that users correctly touched squares larger than $5\text{mm} \times 5\text{mm}$.

A virtual hand can be easily integrated into an existing system using HMD without additional user instrumentation, such as electromagnetic tracking system and/or a data glove. The results showed that using AV-based approach yields a higher visual quality and a more efficient and realistic interaction for the HMD users. ●

A virtual hand can be easily integrated into an existing system using HMD without additional user instrumentation



Figure 7: Traditional visualization of a 3D hand



Figure 8: Visualization of a virtual hand based on augmented virtuality

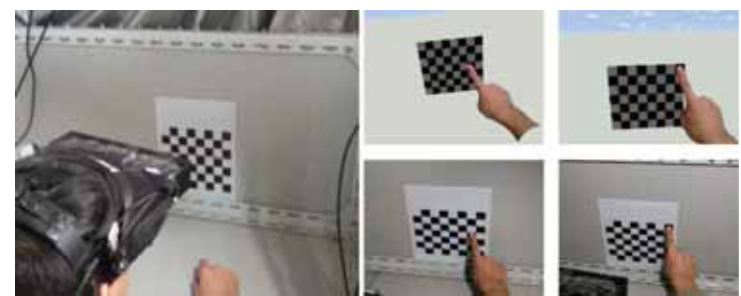


Figure 9: Experimenting with hand inte

ES LIVE

Milton Keynes • 16 May 2013

To register go to www.es-live.co.uk

ES LIVE open its doors on 16th of May 2013, offering electronics design engineers the opportunity to explore cutting-edge technology and electronics innovation at this free exhibition and broad programme of free seminars and practical workshops.

With emphasis on fostering new business relations and growing existing ones, visitors can network with suppliers via the 'Meet the Buyer' area, a quiet, soft-seating area that offers the perfect environment to meet in private with manufacturers, distributors and service providers.

At this year's ES LIVE, there are over 87 exhibitors including Linear Technology, Aerco, Binder, CamdenBoss and Data Modul AG and others.

Visitors are also invited to



Freya Parker, Global events manager at MMG Events



ELECTRONICS SOURCING LIVE
16 MAY 2013
StadiumMK • Milton Keynes
Register now at www.es-live.co.uk

join the LIVE debate called '*In the future, who will run purchasing – designers or procurement professionals?*'

2012 was the year that both device manufacturers and distribution companies unveiled the first generation of new Internet-based software applications designed to bridge the gap between computer-aided design and e-commerce. For the first time, as designs for new electronic products evolved on the computer screen, software was simultaneously building bill-of-materials, sourcing suppliers, checking availability and identifying pricing. So who will run this new empire? Will designers unknowingly consume the purchasing function; will purchasing muscle-in on the design role; or will the concept simply fail. The debate will provide answers to these and other questions of interest now.

"To engineer the products of the future, designers are constantly searching for new electronic component innovations. With leading device manufacturers, distributors and service providers packing the exhibition halls and seminar rooms, ES LIVE is a goldmine of new ideas," said Freya Parker (pictured), Global events manager at MMG Events.

ES LIVE takes place at Milton Keynes. It offers free entry, free car parking, free refreshments, free workshops and even free stadium tours. To register go to www.es-live.co.uk

The Perfect Connector...?

Take the opportunity to decide if Binder's low-cost Snap-in IP67 connectors are the perfect balance of price and performance?

Simple low-cost all plastic modular design

- Cable connectors & moulded cables with up to 12 poles
- Sockets with solder and dip-solder contacts to 7A & 250V

IP67 Snap-in locking mechanism

- Fast, convenient & reliable with over 500 mating cycles
- Internal seals provide water & dust protection

Two compact and lightweight sizes

- Sub-miniature series 620
- Miniature series 720

Versatile Options

- Colour coded versions
- Adaptors for flush mounting

The perfect connector...?

... You decide with your free sample from :

www.binder-connector.co.uk

01442 257339



binder UK

Unit D, ATA House, Boundary Way,
Hemel Hempstead, Hertfordshire HP2 7SS
Tel: 01442 257339 Fax: 01442 239545
sales@binder-connector.co.uk www.binder-connector.co.uk



Tel. 01298 70012
www.peakelec.co.uk
sales@peakelec.co.uk

Atlas House, 2 Kiln Lane
Harpur Hill Business Park
Buxton, Derbyshire
SK17 9JL, UK

Follow us on twitter
for tips, tricks and
news.
@peakatlas

For insured UK delivery:
Please add £3.00 inc VAT
to the whole order.
Check online or
give us a call for
overseas pricing.

PEAK
electronic design ltd

LCR40



£89.95
£74.96+VAT

The Atlas LCR (Model LCR40) is now supplied with our new premium quality 2mm plugs and sockets to allow for greater testing flexibility. Includes 2mm compatible hook probes as standard, other types available as an option.

Automatically test inductors (from 1uH to 10H), capacitors (1pF to 10,000uF) and resistors (1Ω to 2MΩ). Auto-range and auto component selection.

Automatic test frequency from DC, 1kHz, 15Hz and 200kHz.
Basic accuracy of 1.5%.
Battery and user guide included.

DCA75

DCA Pro

"A very capable analyser"
Detailed review in RadCom magazine (March 2011)



Exciting new generation of semiconductor identifier and analyser. The DCA Pro features a new graphics display showing you detailed component schematics. Built-in USB offers amazing PC based features too such as curve tracing and detailed analysis in Excel. PC software supplied on a USB Flash Drive. Includes Alkaline AAA battery and comprehensive user guide.



Now Shipping
£115.95
£96.62+VAT

ESR70



£93.95
£78.29+VAT

The Atlas ESR PLUS (Model ESR70) is designed for testing the true condition of your capacitors.

The ESR70 will measure both the capacitance and internal resistance (equivalent series resistance) with a resolution of 0.01Ω. ESR can even be measured in-circuit in most circumstances.

Features audible alerts and automatic analysis when the probes are applied to a capacitor.

Fitted with new premium quality gold plated 2mm plugs and sockets to allow for different probes. Supplied with gold crocs as standard, other types available. Capacitance from 1uF to 22000uF, ESR from 0.00Ω to 40.0Ω.

DCA55



The Atlas DCA (Model DCA55) is great for automatically identifying your semiconductors, identifying pinouts and measuring important component parameters.

Just connect any way round to automatically detect MOSFETs, Bipolar Transistors, Darlingtons, Diodes, LEDs and more.

Measure transistor gain, leakage current, threshold voltages and pn voltage drops.

Now with sturdy premium probes, really tough and really universal.

Battery and user guide included.

£49.95
£41.63+VAT

It's only possible to show summary specifications here. Please ask if you'd like detailed data. Further information is also available on our website. Product price refunded if you're not happy.

SPECIAL OFFERS
for full sales list
check our website

www.stewart-of-reading.co.uk

Check out our website, 1,000's of items in stock.

Used Equipment – **GUARANTEED**
All items supplied as tested in our Lab
Prices plus Carriage and VAT

AGILENT	E4407B	Spectrum Analyser – 100HZ-26.5GHZ	£6,500	MARCONI	2955	Radio Comms Test Set	£595
AGILENT	E4402B	Spectrum Analyser – 100H-3GHZ	£3,500	MARCONI	2955A	Radio Comms Test Set	£725
HP	3325A	Synthesised Function Generator	£250	MARCONI	2955B	Radio Comms Test Set	£850
HP	3561A	Dynamic Signal Analyser	£800	MARCONI	6200	Microwave Test Set	£2,600
HP	3581A	Wave Analyser – 15HZ-50KHZ	£250	MARCONI	6200A	Microwave Test Set – 10MHZ-20GHZ	£3,000
HP	3585A	Spectrum Analyser – 20HZ-40MHZ	£995	MARCONI	6200B	Microwave Test Set	£3,500
HP	53131A	Universal Counter – 3GHZ	£600	IFR	6204B	Microwave Test Set – 40GHZ	£12,500
HP	5361B	Pulse/Microwave Counter – 26.5GHZ	£1,500	MARCONI	6210	Reflection Analyser for 6200 Test Sets	£1,500
HP	54502A	Digitising Scope 2ch – 400MHZ 400MS/S	£295	MARCONI	6960B with 6910 Power Meter	£295	
HP	54600B	Oscilloscope – 100MHZ 20MS/S from	£195	MARCONI	TF2167	RF Amplifier – 50KHZ-80MHZ 10W	£125
HP	54615B	Oscilloscope 2ch – 500MHZ 1GS/S	£800	TEKTRONIX	TDS3012	Oscilloscope – 2ch 100MHZ 1.25GS/S	£1,100
HP	6030A	PSU 0-200V 0-17A – 1000W	£895	TEKTRONIX	TDS540	Oscilloscope – 4ch 500MHZ 1GS/S	£600
HP	6032A	PSU 0-60V 0-50A – 1000W	£750	TEKTRONIX	TDS620B	Oscilloscope – 2+2ch 500MHZ 2.5GHZ	£600
HP	6622A	PSU 0-20V 4A twice or 0-50v2a twice	£350	TEKTRONIX	TDS684A	Oscilloscope – 4ch 1GHZ 5GS/S	£2,000
HP	6624A	PSU 4 Outputs	£350	TEKTRONIX	2430A	Oscilloscope Dual Trace – 150MHZ 100MS/S	£350
HP	6632B	PSU 0-20V 0-5A	£195	TEKTRONIX	2465B	Oscilloscope – 4ch 400MHZ	£600
HP	6644A	PSU 0-60V 3.5A	£400	TEKTRONIX	TFP2A	Optical TDR	£350
HP	6654A	PSU 0-60V 0-9A	£500	R&S	APN62	Synthesised Function Generator – 1HZ-260KHZ	£225
HP	8341A	Synthesised Sweep Generator – 10MHZ-20GHZ	£2,000	R&S	DPSP	RF Step Attenuator – 139db	£400
HP	8350B with 83592a	Generator – 10MHZ-20GHZ	£600	R&S	SME	Signal Generator – 5KHZ-1.5GHZ	£500
HP	83731A	Synthesised Signal Generator – 1-20GHZ	£2,500	R&S	SMK	Sweep Signal Generator – 10MHZ-140MHZ	£175
HP	8484A	Power Sensor – 0.01-18GHZ 3nW-10uW	£125	R&S	SMR40	Signal Generator – 10MHZ-40GHZ with options	£13,000
HP	8560A	Spectrum Analyser synthesised – 50HZ -2.9GHZ	£2,100	R&S	SMT06	Signal Generator – 5KHZ-6GHZ	£4,000
HP	8560E	Spectrum Analyser synthesised – 30HZ-2.9GHZ	£2,500	R&S	SW085	Polyscope – 0.1-1300MHZ	£250
HP	8563A	Spectrum Analyser synthesised – 9KHZ-22GHZ	£2,995	CIRRUS	CL254	Sound Level Meter with Calibrator	£60
HP	8566A	Spectrum Analyser – 100HZ-22GHZ	£1,600	FARNELL	AP60/50	PSU 0-60V 0-50A 1KW Switch Mode	£250
HP	8662A	RF Generator – 10KHZ-1280MHZ	£1,000	FARNELL	H60/50	PSU 0-60V 0-50A	£500
HP	8672A	Signal Generator – 2-18GHZ	£500	FARNELL	B30/10	PSU 30V 10A Variable No meters	£45
HP	8673B	Synthesised Signal Generator – 2-26GHZ	£1,000	FARNELL	B30/20	PSU 30V 20A Variable No meters	£75
HP	8970B	Noise Figure Meter	£995	FARNELL	XA35/2T	PSU 0-35V 0-2A twice Digital	£75
HP	33120A	Function Generator – 100 microHZ-15MHZ	£395	FARNELL	LF1	Sine/sq Oscillator – 10HZ-1MHZ	£45
MARCONI	2022E	Synthesised AM/FM Sig Generator – 10KHZ-1.01GHZ	£395				
MARCONI	2024	Synthesised Signal Generator – 9KHZ-2.4GHZ	from £800				
MARCONI	2030	Synthesised Signal Generator – 10KHZ-1.35GHZ	£950				
MARCONI	2305	Modulation Meter	£250				
MARCONI	2440	Counter20GHZ	£395				
MARCONI	2945	Comms Test Set various options	£3,000				

STEWART OF READING

17A King Street, Mortimer, Near Reading, RG7 3RS
Telephone: 0118 933 1111 • Fax: 0118 933 2375

9am – 5pm, Monday – Friday

Please check availability before ordering or **CALLING IN**

PCIM Europe 2013

International Exhibition and Conference for Power Electronics, Intelligent Motion, Renewable Energy and Energy Management

Nuremberg, 14 – 16 May 2013

PCIM
EUROPE



International Exhibition and Conference for Power Electronics, Intelligent Motion, Renewable Energy and Energy Management

PCIM is Europe's leading meeting-point for specialists in the field of power electronics and its applications in intelligent motion, renewable energy and energy management. This year, the exhibition boasts 370 exhibitors on 18,500 square meters, and an accompanying program with plenty of new features. Highlights include panel discussions, roundtables, direct access to VIPs, a focus area on energy storage (which lays the foundation for the mapping of the battery technology in power electronics), ECPE joint stand with electric buggies and electric sports cars, and a focus on the job market of semica.

Last year there were 365 exhibitors representing a growth of 19% with the number of visitors exceeding 6,800. The positive growth in the power electronics sector during 2012 was seen in this growing number of exhibitors and space. In addition, some 744 participants attended the seminars, tutorials and conference.

This year, the exhibition will be held in Halls 7 and 9 for the first time, to take into account the growing demand for space from existing exhibitors, as well as an increasing number of new ones. In the last three years alone, the exhibition area of the PCIM Europe grew by 30%.

Best Prospects for 2013

From 14th to the 16th of May all the major companies in the field of power electronics will present their latest innovations in Nuremberg. The future markets of renewable energy, smart grid, energy efficiency and consumer electronics sectors will play a major role. Power electronics are of considerable importance as they are a key technology for many fields of application.

New this year is the second Forum, which will link cross-sector topic areas and offer panel discussions, roundtables, short

seminars and other highlights. In addition, this is where vendor presentations by exhibitors will take place as in past years.

Delegates can expect a total of more than 230 presentations and poster displays in over 40 sessions, providing a comprehensive overview of the most up-to-date power electronics topics. Experts from leading companies as well as colleges and research institutes will reveal their latest findings.

Highlights at the beginning of each conference day will be the keynote speeches on: "HVDC – State of the Art and Future Trends", "New Generation of Traction Drives based on SiC Power Components" and "High-density Fast-transient Voltage Regulator Module", led by first-rate speakers from Siemens, Alstom and Virginia Polytechnic Institute and State University.

Comprehensive Seminars and Tutorial Programs

Six seminars and ten tutorials will offer delegates the opportunity to learn more about different power electronics topics. These will be led by specially invited internationally-renowned industry experts who will speak on issues in their own specialist areas.

The detailed conference program and an up-to-date exhibitor can be found at: <http://www.mesago.de/en/PCIM/>

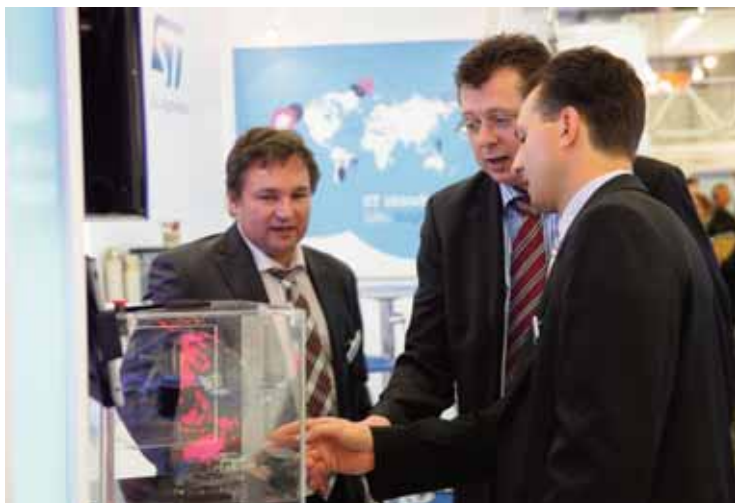
PCIM Europe covers products and services in the following fields:

- Power Semiconductors
- Passive Components
- Magnetic- and Core Materials
- Thermal Management
- Sensors
- ASICs
- Micro-Controller Servo-Technology/Actuators
- DSPs, Microprocessors
- Power Supplies, UPS
- Energy Storage and Distribution Systems
- Energy Management
- Software
- Test & Measurement Equipment

Free entry tickets

Get your free entry ticket by registering online. Visit PCIM Europe's website at www.pcim-europe.com/tickets for access to the most comprehensive event of the power electronics industry.

More about the PCIM Europe Conference can be found at www.pcim-europe.com/conference.



University of Oxford

Technology Programme June / July 2013

Short courses for professional engineers



- **Digital Engineering**
- **EMC & Signal Integrity**
- **Electronics**
- **Telecoms & Mobile**

Courses include:

- High-Speed Digital Design
- PCB Design for Real-World EMI Control
- Advanced EMC & Signal Integrity
- Practical RF / Microwave Design
- RF PCB Design
- Practical Antenna Design: Theory & Practice
- Digital Signal Processing
- LTE & LTE-Advanced: System Design
- White Space Networks for M2M Services



For more information, or to book a place:

T: +44(0)1865 286958

E: technology@conted.ox.ac.uk

W: www.conted.ox.ac.uk/ew13



bulgin

a brand of Elektron Technology



The new Bulgin 6000 Series connector

Robust, instant connections for harsh environments

Bulgin's new 6000 Series of waterproof power and data connectors have a quick and easy-to-use push-pull latching system with unique locking facility for fast and reliable connections. And they look good too!

Designed to meet IP66, IP68 and IP69K standards, the 6000 Series combines an easy-to-use push-pull mechanism with proven environmental sealing in a compact package, giving engineers a choice of power and data connections in a practical selection of body styles.

The 6000 Series is designed for long-term exposure in both harsh outdoor environments, where prevention of water ingress is critical, as well as demanding interior environments such as factory floors, where dust can be a problem. Its innovative design makes it ideal for any application where ease of connection, ease of use, space and appearance are important considerations.

Technical Specification

- Push-pull latching with unique 30° twist lock
- 2, 3, 8, 16 and 22 poles – ratings up to 16A, 277V
- USB V2.0 and ethernet (RJ45) data interfaces
- cULs, UL, VDE, CCC approvals (pending)
- IP66, IP68 and IP69K environmental sealing
- Temperature range: -40 to +120°C
- All plastic version: UL94-V0 rated, UV-stable, halogen free
- Metal body version: CNC-machined brass, nickel-plated

To find out more or to request a sample please contact:

t: +44 (0)1803 407752

e: connectivity@elektron-technology.com

w: bulgin.com





Staying On Top of The Manufacturing's Beat

BY REG WALLER, EUROPEAN DIRECTOR, ASSET INTERTECH INC

Electronic manufacturing engineers talk about the beat rate – the rate at which product, such as a circuit board, is produced – as if it were the factory's heart rate. Well, it is. But most doctors will tell you that a normal heart rate can mask underlying health issues.

On the manufacturing floor, issues hazardous to the health of the production line are sometimes caused by variances in manufacturing processes. If undetected, these variances can lead to boards that won't pass the final test, or if they do, failures in the field, followed by excessive warranty returns. Either way the manufacturing puts its fiscal health at risk.

This can be particularly critical these days as the data transfer rates on chip-to-chip serdes (serializer/deserializer) transmission lines continue their seemingly inevitable upward climb. At the accelerated rates of serdes links like PCI Express, the DDR3 or DDR4 memory bus, Intel's QuickPath Interconnect (QPI) and others, the physical

characteristics of a trace on a circuit board have to be spot on or the serdes may not perform to specification.

Consequently, the manufacturing engineer faces a delicate balance. Keep the beat rate healthy, but don't sacrifice product quality by failing to detect process variances.

A Variety of Variances

The defects caused by process variances come in a variety of shapes and sizes. Figure 1 shows just some of them. Traces on boards may look fine one day and have one or more of these defects the next. Any one of these defects may or may not have an impact on serdes performance, since most designs are developed with a certain level of confidence in their operating margins, but the cumulative effects of several defects may downgrade the performance of a serdes. In addition, identifying a process that is heading towards 'out-of-spec' could give the manufacturer a chance to correct the problem before it becomes disastrous.

Historically, performance on serdes lines has usually been validated on prototype boards because that was when designers had the time to pull out the old oscilloscope and validate the design. Today's high-speed serdes are different, however. Because of higher signal frequencies, placing a probe on a serdes introduces anomalies into the signal that can invalidate the test data. Equally, trying to put a scope on every trace during manufacturing would certainly impede the beat rate.

Seeing What The Receiver Sees

Although validating serdes performance for every board that's manufactured and during every phase of the life cycle would be the ideal solution, the real-world demands and challenges of high-volume manufacturing make such a proposition all but impractical. However, there are new techniques that test from the inside out and which can be applied effectively to selected sample lots of boards during manufacturing.

Margining tests – tests which validate that the serdes is executing within its operating margins – and bit error rate (BER) tests can be applied through instrumentation

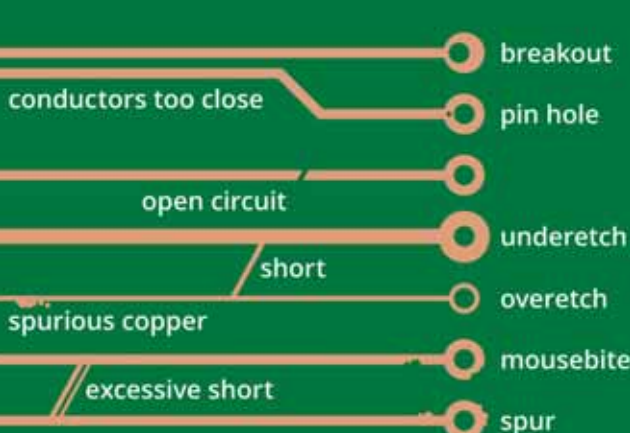


Figure 1: Some defects caused by process variances

All too often in today's hyper-competitive world of low profit margins, signal integrity validation is neglected

embedded in the on-board chips on sample lots of boards to uncover manufacturing variances. Unlike oscilloscopes and vector network analyzers, margin and BER tests generated by embedded instruments do not require the time consuming setup or specialized operator expertise that can wreak havoc on the beat rate. If the board has been designed with a modicum of concern for test, you may be surprised by its internal test capabilities.

One of the big advantages of some implementations of embedded instrumentation is it can monitor serdes performance at the receiver and report test results to a software-driven external test platform. Cumbersome and less-than-effective external fixtures are avoided. In some cases, the instrumentation embedded in a board's chips can also detect structural and functional faults.

Intel has become a major proponent of embedded

instrumentation. In fact, its three main families of chips – Core, Atom and Xeon – all have extensive embedded instrumentation technology in silicon. There are also a number of industry standards and initiatives that are laying the foundations for an embedded instrumentation ecosystem.

In many cases, the IEEE 1149.1 boundary-scan (JTAG) standard provides access to these embedded instruments. An addition to the JTAG family of standards, IEEE P1687 Internal JTAG (IJTAG), will standardize the way engineers manage, control and operate embedded instruments.

At the end of the day, it looks like attention to the beat rate and the ability to validate serdes performance are not as mutually exclusive as we might have thought. ●

FURTHER READING

IF YOU'D LIKE TO LEARN MORE ABOUT THIS TOPIC, THERE'S A NEW E-BOOK AVAILABLE AT: <http://www.asset-intertech.com/Products/High-Speed-I-O-Validation/HSIO-Software/Manufacturing-Variance-e-Book>

RELIABLE LOW POWER RADIO MODEMS FOR PERFORMANCE CRITICAL APPLICATIONS



ASCII in, ASCII out, 9600 baud wireless link, minimum effort

- Takes care of all over-air protocols
- European license-free 433 MHz ISM band & Custom frequencies
- Line-of-sight range over 500m
- Transmit power: +10dBm (10mW)
- Receiver sensitivity: -107dBm (for 1% BER)
- Addressable point-to-multipoint
- Conforms to EN 300 220-3 and EN 301 489-3
- No additional software required

Ideally suited for fast prototyping / short design cycle time

TXL2 & RXL2



Producing VHF and UHF, ISM band modules for over 25 years.

T: +44 (0) 20 8909 9595 sales@radiometrix.com
www.radiometrix.com

 **RADIOMETRIX**
WIRELESS DATA TRANSMISSION



Four-Channel LED Driver IC For Automotive Interior Lighting

The new A6263 is the latest addition to the family of automotive qualified LED driver ICs from Allegro MicroSystems Europe.

The new device incorporates a linear programmable current regulator providing up to 100mA from each of four outputs to drive arrays of high brightness LEDs. It is targeted at the automotive market for applications such as map and dome lighting, as well as exterior accent lighting.

The device outputs can be connected in parallel or left unused as required. The regulated LED current from each output is set by a single reference resistor. Current is matched in each string without the use of ballast resistors. Driving LEDs with constant current ensures safe operation with maximum possible light output.

The A6263 incorporates protection against a range of common faults, including LED string shorted to ground, single or multiple LED shorts, LED string open, IC pin open or short and over-temperature.

www.allegromicro.com

NEW KONTRON STARTER KIT FOR EMBEDDED HIGH-END GRAPHICS

Kontron announced its new COM Express Starterkit Reference T6 for the accelerated development of a broad range of small form factor (SFF) multimedia applications, providing a rich user experience ranging from battery-powered portable solutions up to stationary multi-display installations.

Following the launch of the Kontron COM Express Starterkit Eval T6, the new Reference T6 Starterkit was compiled specifically for OEMs who need to design fully-featured SFF applications using COM Express.

The starter kit provides a space efficient Mini-ITX sized carrier board that can host any COM Express pin-out Type 6 Computer-on-Modules in the basic (125 x 95mm) and compact (95 x 95mm) form-factors for most flexible performance scalability. The starter kit is specifically configured to enable the quick evaluation and development of graphics-intensive solutions using the latest interfaces such as DisplayPort, HDMI, DVI or LVDS in Mini-ITX sized designs. With SIM card support, it also enables always-connected and constantly updated ubiquitous distributed solutions.

www.kontron.com



NEW HMO3000 MIXED SIGNAL OSCILLOSCOPE SERIES FROM HAMEG INSTRUMENTS

There are six new model variants in the new HMO3000 series by Hameg Instruments, available in a bandwidth of 300MHz to 500MHz with two or four channels. The standard MSO functionality allows you to analyze the analog channels plus up to an additional 16 digital channels.

Another significant difference to the previous series is the memory depth of 8MB, which offers twice the capacity and is manually and automatically adjustable.

In addition, there's an upgrade possibility which allows all models of the HMO3000 series with 300MHz or 400MHz to be expanded to a bandwidth of 500MHz: for 300MHz models with the options H00352 (2 channels) and H00354 (4 channels), and for 400MHz models with the options H00452 (2 channels) and H00454 (4 channels).

As an introductory offer all oscilloscopes of the HMO3000 series will be shipped with the logic probe H03508 included at no extra cost. This offer is valid until the 31st of October 2013.

www.hameg.com

NEW KIKUSUI PWX SERIES PROGRAMMABLE DC POWER SUPPLY

The PWX series is a CVCC programmable regulated DC power supply designed for a rack-mounted or bench use. To increase its mounting efficiency, it has a 19-inch rack width which is only 1U high with cooling running from the front to the back which means units can be stacked on top of each other. The series is equipped standard with USB, RS-232C and LAN interfaces, which are essential for system upgrades. The series also has a virtual multi-channel bus (VMCB) function that allows it to be used efficiently for remote control and monitoring with 1-to-N and as well as with N-to-M in large-scale networks. In particular, the LAN interface is LXI compliant, enabling you to control and monitor the power supply easily from a browser on a PC, smartphone, or tablet. You can also manage the power supply in a different building.

www.telonic.co.uk



BBP85 SIGN AND LABEL PRINTER FOR LARGE FORMAT, MULTICOLOUR PRINTING

Brady introduces the BBP85 sign and label printer, its new large-format, multi-colour thermal transfer printer.

The BBP85 printer has an exceptionally easy-to-use touch-screen interface and can print multicoloured signs and labels up to 254mm wide. Combined with Brady materials that last in challenging indoor conditions and up to 10 years outdoors, the BBP85 sign and label printer offers the

optimal in-house printing



solution for custom safety and facility identification.

The new printer comes with Brady's fastest, easiest operating system to date. Its touch-screen interface makes label design fast, simple and accessible. It is also pre-programmed with convenient applications for creating common visuals such as pipe markers, CLP/GHS labels and chemical signs.

The BBP85 printer also offers an extensive list of advanced design and print capabilities. It has over 300 built-in symbols, hundreds more pictograms, three barcode symbol sets and 11 operating languages.

www.bradyeurope.com

Harting Introduces har-Speed M12 Connector Incorporating Moulded Interconnect Device (MID) Technology

Harting has expanded its har-speed range of connectors with a new PCB connector which will be manufactured using moulded interconnect device (MID) technology.



A straight variant for PCB connection will initially be launched on the market.

Using MID technology means that the size of the new connector has been significantly reduced compared to a conventional PCB connector. The new addition to the M12 range is intended for the integration of the M12 connector configuration into high-speed communication devices such as switches and routers.

Shielding inside the connector is redefined with MID technology. The metal shielded cross is now superfluous. Two plastics are used in the 2-shot MID process, one of which can be deployed with a surface coating in a plating process. The new connector is significantly lighter, with a weight reduction of around 30% per component, and like the larger conventional device can be soldered onto the circuit board in the reflow process.

www.harting.com

AVX Introduces Ultra-Broadband Capacitor Series

AVX has introduced a new ultra-broadband capacitor series, designed to address DC blocking from 16kHz to 40GHz.



The new GX03 series ultra-broadband capacitors exhibit ultra-broadband performance, extremely low insertion loss, excellent return loss and X7R characteristics. Ideal applications for the GX03 series include semiconductor data communications, receiver optical subassemblies, transimpedance amplifiers and test equipment.

"The GX03 series was specifically developed for applications that require higher voltages than accommodated by our other broadband capacitor offerings," said Larry Eisenberger, Senior Marketing Application Engineer at AVX.

Rated at 50VDC from -55°C to +125°C, the new GX03 series ultra-broadband capacitors feature a 0603 case size, are completely orientation insensitive, and utilize AVX's patented, precision, thin film termination process to minimize board space requirements.

Available with Ni-Sn and Ni-Au terminations, AVX's GX03 series capacitors are compatible with a wide range of attachment processes, including wire bonding for Ni-Au terminated components.

www.avx.com

NEW 3A ULTRA-LOW DROPOUT LINEAR REGULATOR FROM ADVANCED POWER ELECTRONICS CORP

Advanced Power Electronics Corp (USA), a leading Taiwanese manufacturer of MOS power semiconductors for DC-DC power conversion applications, has introduced the APE8968MP-HF3, a new series of 3A, ultra-low dropout linear regulators designed to provide simple POL DC-DC conversion in board-level applications, including motherboard and notebook applications. Requiring two supply voltages – one for the control circuitry and the other for the main supply – the IC reduces power consumption and provides a dropout of just 0.23V (typ) at 3A.



APE8968MP-HF3 integrates many functions and has a Power-On-Reset (POR) circuit to monitor both supply voltages to prevent incorrect operation. Thermal shutdown and current limit protection features are included, and a POK indicates output status with a time delay which is set internally. The APE8968MP-HF3 can control another converter for power sequencing, and can also be controlled by another power system. Pulling and holding the EN pin below 0.4V shuts off the output.

www.a-powerusa.com

ITT'S INTERCONNECT SOLUTIONS BUSINESS LAUNCHES ENHANCED WEBSITE

ITT Corporation announced its Interconnect Solutions business has launched an enhanced website at www.ittcannon.com that offers its customers and other users a variety of features that improve the usability, functionality and performance of the site.

New features include an updated design, the ability to easily search products and part numbers, improved product descriptions and specifications, and a new product catalog library. Other enhancements include the ability to configure part numbers, download select two-dimensional drawings and three-dimensional models, and download data sheets for individual part numbers.

"The Interconnect Solutions team is committed to enhancing our capabilities to better serve our customers, and this website is just one example of our continuing efforts to provide a premier customer experience," said ITT's Interconnect Solutions VP of marketing, Anh Phan. "Our goal was to re-imagine our site from a customer's point of view, and we are now offering a fresher, more engaging and user-friendly site."

www.ittcannon.com



HIGH-EFFICIENCY DC-DC BOOST CONVERTER BASED ON A GALLIUM NITRIDE SWITCH

Arkansas Power Electronics International (APEI) and GaN Systems have tested a DC-DC boost converter that's based on the ultra-high switching capability of GaN Systems's high power switch to achieve a 1MHz switching capability. The boost converter showed 98.5% efficiency at 5kW output power, with turn-on and turn-off transitions of only 8.25ns and 3.72ns, respectively.

The converter shows efficiency, performance and reliability of gallium nitride power devices required in hybrid and electric vehicles (HEVs and EVs), as well as high-efficiency power supplies, solar inverters and industrial motor drives.

Gallium nitride power switches offer increased system performance advantages over traditional power semiconductor devices when used in power conversion systems. "Wide bandgap semiconductor technology, such as gallium nitride, enables increased power density for modern power electronic systems," said Dr. Ty McNutt, Director of Business Development at APEI. "We are excited to be developing novel power packages and high performance systems around these ultra-high speed devices."

www.gansystems.com



IC Design Consultancy Sondrel completes Third Successful 28nm Tape-Out

Sondrel, a system-to-silicon IC design consultancy, has just completed its third 28nm design this year for a leading communications company, and is closing on two more at this node. Although Sondrel has worked on over 200 IC designs at all nodes down to 20nm and chip sizes over 700mm².

The fact that the company has so many successful tape-outs at 28nm convinces CEO Graham Curren that 28nm will be the

preferred geometry for complex chips for some time to come: "As an independent design consultancy we have

customers in all sectors – mobile, computing, graphics, consumer, automotive – so it is interesting that so many of our projects are based around 28nm. We think this is perhaps because 28nm appears to be a strong, stable process with good yield and performance characteristics, and is therefore more attractive than 40nm or the still new 20nm node."

www.sondrel.com



HARWIN'S HI-REL CONNECTOR FAMILIES ENTER THE STRATOSPHERE

Harwin has congratulated the team at Warwick University on the successful launch and recovery of the maiden flight of the WUSAT nano-satellite, which has used Harwin's high reliability Datamate and Gecko connector families to provide signal and power connection.

The university team launched a 'CubeSat' – a small satellite typically measuring just 10 x 10 x 10cm, with a mass of up to 1.33kg, with the goal to open up many new possibilities for payloads and further development. The team has based control, power and communications systems on the Arduino platform for speed of development. Data from sensors included on separate PCBs was captured on SD cards.



With this level of systems payload, a miniature and lightweight yet very high-reliability interconnect system was required, so the WUSAT team has been evaluating Harwin's 2mm Datamate signal and power connector family, and its recently-launched 1.25mm Gecko connector range that can handle up to 2A. Both connector families perform well in harsh environments.

www.harwin.co.uk

RAINBOW BRINGS A NEW DIMENSION TO DISPLAYS

PCB technology company Rainbow Technology Systems has developed a revolutionary new method for manufacturing touchscreen displays which it says is more cost-effective, faster and greener than traditional methods.

The Rainbow Process Unit has been developed for primary imaging of PCB inner layers, but the technology can be equally applied to touchscreen displays where it is capable of producing very fine line circuitry (down to five micron detail levels). Central to the success of the Rainbow process is the proprietary liquid etch resist which does not require pre-drying (using a hot air or infra-red oven) before imaging. The resist is 100% solids and completely solvent-free.

Rainbow can produce grid patterns with, for example, five micron copper lines in a hexagonal pattern at 300-micron pitch, offering more conductivity than ITO or conductive polymers with extremely good transparency. The process can be done additively using an imaged seed layer.

www.rainbow-technology.com



RS Launches New Feature-Rich Designspark

PCB Version 5.0

RS Components (RS) has unveiled the latest release of DesignSpark PCB, the company's award-winning professional software for schematic capture and PCB layout. DesignSpark PCB Version 5.0 integrates two additional features within the free design tool – online Design Rule Checking and buses – which have been introduced to further reduce design times for engineers and to minimise errors during the design process.

This new release builds upon the previous version of DesignSpark PCB announced in October 2012, which provided access to the industry-leading ModelSource component library, PCB quote service and BOM quote functionality.

Design Rule Checking determines whether the physical layout of an integrated circuit satisfies a series of recommended parameters called design rules. DRC is an important step during the physical verification of a design, which is normally carried out in the post-design phase. Online DRC is an advancement of this process that enables the engineer to detect errors in real-time during the design stage.

www.rs-components.com

KEMTRON PUBLISHES A COMPREHENSIVE NEW CATALOGUE

UK manufacturer of RFI/EMI shielding solutions Kemtron has published a comprehensive new catalogue in response to customer demand. The 144-page printed catalogue has proved popular with customers who have limited Internet access, or who prefer the convenience of a paper version that they can bookmark, add notes or use as a working reference tool.

"We have had a fantastic response from customers in countries like Germany, India and Turkey, as well as the UK. They welcome the fact that they can have a printed catalogue when so many suppliers only offer information on the Web," said David Wall, Kemtron's Managing Director.

The catalogue provides detailed product overviews, technical specifications, application information and design considerations for Kemtron's range of RFI/EMI shielding solutions, as well as background information on EMC and useful design tools.

www.kemtron.co.uk

Mouser Now Stocking the World's First Round LED from Luminus Devices

Mouser Electronics is stocking the world's first round LED, the CBT-140 Big Chip Round LEDs from Luminus Devices. This new round emitting aperture provides the most efficient match for circular optical systems and narrow beam projectors.

Luminus Devices CBT-140 Big Chip Round LEDs & Modules are the perfect solution for applications defined by a circular aperture. Such optical architectures, previously mismatched with a traditional square LED, can now be updated with round LEDs which better match the application. The Big Chip Round LEDs & Modules increase system-level efficiency by as much as 30%, enabling customers to use a single LED to replace a 250W HID lamp. They will accelerate the adoption of solid-state technology by displacing conventional light sources in high brightness lighting applications.



www.mouser.com

NEW CONNECTORS FROM BINDER ARE IP67 UNMATED

A new connector system from Binder has a design that protects the contacts to IP67 when not connected, without the need of a protective cap. Originally designed for medical equipment, the Binder 770 Series NCC (non-connected closed) range will also prove ideal for all types of portable or handheld measuring equipment, control devices and other applications where it is an advantage to make rapid set-up changes. The efficiency of the design achieves a product life in excess of 5,000 mating cycles.

Series 770 is a panel-mount receptacle in which the electrical contacts are protected from water, dust and foreign particles by a spring-mounted lid when unmated. When the cable plug is mated the contact cover is pushed inside the receptacle body, the contacts engage and the connector is locked with a quarter turn of a bayonet-locking collar. The connectors have eight gold-plated contacts and are rated to 2A and 175V.

www.binder-connector.co.uk



CCLIX
perfectly
into place

LOW COST Industrial Computer
INSTANT Start up
MQX Real Time Operating System
POWERFUL Development Tools
SOURCE Level, Task Aware Debugging
OVER 30 yrs of UK support for clients

Check out our Website for full details:

www.CCLIX.co.uk

The perfect place for answers



CAMBRIDGE MICROPROCESSOR SYSTEMS LTD
Unit 17 Zone 'D' Chelmsford Road Industrial Estate,
Great Dunmow, Essex UK CM6 1XG

Digital Oscilloscope

DS1000E Series



2 Channels
50-100MHz BW
1GSa/s Sample Rate
USB

From £239 + VAT

TELONIC
www.telonic.co.uk
Tel: 01189 786 911

RIGOL
www.RIGOL-UK.CO.UK

Industrial MEMORY
SOLUTIONS

www.apacer.com

Industrial SSD
SOLUTIONS

embedded@apacer.nl

To advertise
in this section
contact
Orla Cullen
Tel: +44 (0)207 933 8985
orlac@sjpbusinessmedia.com

**Electronics
WORLD**

TELONIC
www.telonic.co.uk

PROGRAMMABLE DC POWER SUPPLIES 2 - 900kW



**MAGNA-POWER
ELECTRONICS**

Tel: 01189786911 • Fax: 01189792338
www.telonic.co.uk • info@telonic.co.uk



PIC10F222-I/P	0.35	PIC16F1934-I/PT	0.93
PIC12F508-I/SN	0.26	PIC16F1939-I/PT	1.21
PIC12F508-I/P	0.31	PIC18F1220-I/SO	1.35
PIC12F629-I/SN	0.42	PIC18F4520-I/PT	2.21
PIC12F675-I/SN	0.43	PIC18F8720-I/PT	5.12
PIC12F683-I/SN	0.55	PIC18F8722-I/PT	4.35
PIC16F616-I/P	0.66	PIC18F45K22-I/PT	1.25
PIC16F630-I/P	0.49	PIC18F67K22-I/PT	2.11
PIC16F648A-I/P	0.97	ATMEGA8A-16PU	0.81
PIC16F690-I/SS	0.78	ATMEGA8-16AU	0.79
PIC16F690-I/SO	0.85	ATMEGA48A-AU	0.71
PIC16F877A-I/PT	2.31	ATMEGA64A-AU	2.21
PIC16F818-I/SO	0.94	ATMEGA88PA-MU	0.68
PIC16F883-I/SP	0.98	ATMEGA128A-AU	2.89
PIC16F883-I/SO	0.82	27C256B-10F1	1.78
PIC16F886-I/SP	1.08	27C512-10F1	1.95
PIC16F886-I/SO	0.98	27C2001-10F1	2.71
PIC16F887-I/PT	1.16	27C4001-10F1	2.95
PIC16F1823-I/P	0.68	M4A5-32/32-10VNC	2.65
PIC16F1827-I/SO	0.65	M4A5-128/64-10VNC	4.85
PIC16F1933-I/SS	0.72	MAX232CPE+	0.61

We can also supply Maxim/Dallas, Lattice, Linear Tech
PLEASE VISIT OUR WEB SITE FOR FULL LIST

TELONIC **KIKUSUI**
www.telonic.co.uk info@telonic.co.uk

AC POWER SUPPLIES /
FREQUENCY CONVERTERS

DC ELECTRONIC LOADS



ELECTRICAL SAFETY TESTERS

PROFESSIONAL DC POWER
SUPPLIES

Tel: 01189 786 911 Fax: 01189 792 338

swissbit®

INDUSTRIAL MEMORY SOLUTIONS
NAND FLASH PRODUCTS & DRAM MODULES

- Industrial Temperature Grade (-40°C to +85°C)
 - Controlled BOM
 - PCN Process
 - SLC NAND Flash
 - Small Form Factor
- www.swissbit.com



UK SMALL FIRMS NEED THE GOVERNMENT'S SUPPORT

The UK Science & Technology Select Committee believes the government does not have a coherent strategy to support the commercialisation of technological innovation; it states the British entrepreneurs are “badly let down” by lack of financial support.

“Britain has a fine tradition of producing some of the world’s leading technology companies and, yet, it is clear that in these austere times the lack of access to funding has caused a bottleneck that is preventing many companies from growing to their full potential,” said Dermot Campbell, Managing Partner at Kuber Ventures. “At seed level, technology companies receive some support for development through generous incentives. However, the reality is that these companies encounter considerable challenges at round two of the funding process. With options limited to them, technology companies look for alternative investments to help them sustain growth.”

“One of the most significant incentives ends on 5th April 2013, as the absolute saving of Capital Gains Tax on Seed Enterprise Investment Scheme (SEIS) comes to an end. We would like to see an extension of the Capital Gains Tax exemption into the 2013/14 tax year and extended to second-round funding, so both –investors and small businesses – can benefit,” he added. “Thankfully, by level-three funding, the bottleneck improves and programmes such as the Enterprise Investment Scheme (EIS) are on hand to help support future development.”

Technology companies currently make up a significant percentage of the small businesses in the UK involved in the EIS scheme, which continues to be very popular.

PROFESSOR DR DOGAN IBRAHIM, Near East University in Nicosia, Cyprus: Financial support is the key to invention and development of technological products. Britain is well known with many inventions in science and electronics in the past. Without enough financial support most inventions will remain on paper and just gather dust.

I strongly agree that the government should do much more in the next budget to financially support both investors and small businesses engaged in technology.

HAFIDH MECHERGUI, Associate Professor in Electrical Engineering and Instrumentation, University of Tunisia: The financing of small companies is essential, because they contribute to the development of the country’s economy. It is necessary to give these companies the assistance and support they need, providing them with a good stead. Criticisms towards the UK government are constructive, because the UK as industrial leader must have a strategy of clear financing and play a more effective part by reinforcing its assistance to small companies. Measures taken to reduce small companies’ research risk is a big step to help them overcome their financial problems and to ensure their success.

The UK must have a national strategy in place to reinforce its support for companies that innovate, as innovation is one of the main parts of competitiveness and a determining factor for the companies’ profitability and economic growth. In turn this will improve British competitiveness globally.

BARRY MCKEOWN, RF and Microwave Engineer in the Defence Industry, and Director of Datod Ltd, UK: The UK’s Select Committee’s “Bridging the Valley of Death” is a serious undertaking, which essentially critiques the current TSB and Catapult establishment for getting university (and thus primarily public-funded) research into commercial ventures to achieve economic benefits and jobs. The fundamental problem is that this approach is based on a one-sided perception of knowledge flow from universities to industry and not industry to universities.

This is now being recognised. Finance companies like Kuber Ventures are a menace, as they are only interested in cashing out and selling off fledgling technology companies, even when they have a clearly-defined three or more product stage pipeline. They play at risking other peoples’ money. Instead they should be looking for safe havens in coffee shops and restaurants if they are only interested in tax breaks.

In short, if finance companies are not prepared to lose their capital investment and are prepared to just walk away with only nebulous scientific knowledge, my advice is to just ignore them. They have no place in either a disruptive top-down or bottom-up strategy as they are not mentally equipped for the global technological battlefield.

MAURIZIO DI PAOLO EMILIO, Engineer, University of L’Aquila and EDM Engineering, Italy: Science and technology are critical inputs for economic development and poverty alleviation. Advances in science and technology make it possible to reduce poverty and improve quality of life.

In the future, the ability of countries to use scientific and technological knowledge will increasingly be a determining factor of the material well-being and quality of life of their citizens.

The disadvantage of science and technology is that it can be easily manipulated by irresponsible people. When it goes into the wrong hands, it can negatively impact the society, by increased rates in cyber crimes, hacking and stealing personal information, for instance.



In these austere times, the lack of access to funding has caused a bottleneck that is preventing many companies from growing to their full potential

CAD CONNECTED

PCB Layout

Microprocessor Simulation



PROTEUS DESIGN SUITE VERSION 8

Featuring a brand new application framework, common parts database, live netlist and 3D visualisation, a built in debugging environment and a WYSIWYG Bill of Materials module, Proteus 8 is our most integrated and easy to use design system ever. Other features include:

- Hardware Accelerated Performance.
- Unique Thru-View™ Board Transparency.
- Over 35k Schematic & PCB library parts.
- Integrated Shape Based Auto-router.
- Flexible Design Rule Management.
- Polygonal and Split Power Plane Support.
- Board Autoplacement & Gateswap Optimiser.
- Direct CADCAM, ODB++, IDF & PDF Output.
- Integrated 3D Viewer with 3DS and DXF export.
- Mixed Mode SPICE Simulation Engine.
- Co-Simulation of PIC, AVR, 8051 and ARM MCUs.
- Direct Technical Support at no additional cost.

labcenter 
Electronics www.labcenter.com

Labcenter Electronics Ltd. 21 Hardy Grange, Grassington, North Yorks. BD23 5AJ.
Registered in England 4692454 Tel: +44 (0)1756 753440, Email: info@labcenter.com

Visit our website or
phone 01756 753440
for more details

Wall Mounting Uninterruptible Power Supplies for Long Battery Standby Periods



WM800 to WM4000 Series 800VA to 4000VA Rating

The WM800... series of Uninterruptible power supplies are ideal for applications where long battery autonomy is required. Batteries are connected externally and can be typically between 50Ah and 500Ah to give several hours of battery back up or more, depending on the load taken and batteries selected. There are 6 models in the range for 230VAC input and output and 5 models available with 115VAC output. They can be used for long periods under battery only and do not need AC connected to operate from a fully charged battery, so they can be used in applications where an AC supply is required but no AC outlet is available, providing the battery has been fully charged previously. For example in mobile equipment. The AC output is sinusoidal and the UPS is a line interactive design so runs at maximum efficiency when the AC supply is connected. Transfer time is very fast at only 3mS from black out to changeover to inverter. These products also feature smart automatic voltage regulator function for applications such as generators where the AC input can vary widely. For more details check out the full technical specification on our website.

**POWER
SOLVE**

www.powersolve.co.uk

Tel: 01635 521858 Email: sales@powersolve.co.uk